THE JOURNAL OF BIOLOGICAL CHEMISTRY VOL. 291, NO. 35, pp. 18562–18581, August 26, 2016

Misregulation of a DDHD Domain-containing Lipase Causes Mitochondrial Dysfunction in Yeast*

Received for publication, April 18, 2016, and in revised form, June 30, 2016 Published, JBC Papers in Press, July 8, 2016, DOI 10.1074/jbc.M116.733378

Pradeep Kumar Yadav[1] **and Ram Rajasekharan**[2]

From the Lipidomic Centre, Department of Lipid Science and the Academy of Scientific and Innovative Research, Council of Scientific and Industrial Research (CSIR)-Central Food Technological Research Institute (CFTRI), Mysore 570020, Karnataka, India

The DDHD domain-containing proteins, which belong to the intracellular phospholipase A_1 ($iPLA_1$) family, have been predicted to be involved in phospholipid metabolism, lipid trafficking, membrane turnover, and signaling. Defective cardiolipin (CL), phosphatidylethanolamine, and phosphatidylglycerol remodeling cause Barth syndrome and mitochondrial dysfunction. Here, we report that Yor022c is a Ddl1 (DDHD domain-containing lipase 1) that hydrolyzes CL, phosphatidylethanolamine, and phosphatidylglycerol. Ddl1 has been implicated in the remodeling of mitochondrial phospholipids and CL degradation. Our data also suggested that the accumulation of monolysocardiolipin is deleterious to the cells. We show that Aft1 and Aft2 transcription factors antagonistically regulate the *DDL1* gene. This study reveals that the misregulation of *DDL1* by Aft1/2 transcription factors alters CL metabolism and causes mitochondrial dysfunction in the cells. In humans, mutations in the *DDHD1* and *DDHD2* genes cause specific types of hereditary spastic paraplegia (SPG28 and SPG54, respectively), and the yeast *DDL1*-defective strain produces similar phenotypes of hereditary spastic paraplegia (mitochondrial dysfunction and defects in lipid metabolism). Therefore, the *DDL1*-defective strain could be a good model system for understanding hereditary spastic paraplegia.

The DDHD domain was first identified as a long stretch of 180 amino acids in the central part of the Nir/rdgB (N-terminal domain-interacting receptor/*Drosophila* retinal degeneration B) proteins. This domain possesses four conserved amino acid residues (DDHD), and the name DDHD domain is based on these four residues. This domain is also found in the C-terminal region of the phosphatidic acid (PA)[3]-preferring phospholipase A_1 ($PA\text{-}PLA_1$). The DDHD domain has been predicted to be involved in phospholipid metabolism, lipid trafficking, membrane turnover, and signaling (1). The $iPLA_1$ proteins constitute a recently identified lipid-metabolizing enzyme family. $PA\text{-}PLA_1$/DDHD1, KIAA0725p/DDHD2, and p125/Sec23ip are three mammalian $iPLA_1$ family members. Yeasts, nematodes, and plants also have $iPLA_1$ family proteins (2). Higgs and Glomset (3) identified the first $iPLA_1$ member, $PA\text{-}PLA_1$, in bovine brain and testis. The hydrolase activities of DDHD1 and DDHD2 (4, 5) have been studied, whereas that of p125 is yet to be demonstrated. In humans, mutations in DDHD1 cause a type of hereditary spastic paraplegia (HSP) termed SPG28 (6), whereas mutations in DDHD2 cause SPG54 (7). HSP is a genetically and clinically heterogeneous group of inherited neurological disorders. Defects in intracellular membrane trafficking, mitochondrial functions, and lipid metabolism have been associated with HSP pathogenesis (6, 8).

The mitochondria are crucial organelles that control the life and death of the cell. Important metabolic reactions, the synthesis of most of the cellular ATP, and the regulation of a number of signaling cascades, such as apoptosis, occur in the mitochondria (9). The major non-bilayer-forming phospholipids, phosphatidylethanolamine (PE) and CL, are synthesized in the mitochondria (10, 11). The presence of CL and PE is important for mitochondrial fusion (12). In the absence of CL, a reduction in the inner membrane potential $\Delta\psi$ and a defect in protein import into the mitochondria have been reported (13). It has been suggested that CL and mitochondrial PE have overlapping functions and that PE compensates for the loss of CL and vice versa (14). Barth syndrome patients have deficiencies in the molecular species of CL, phosphatidylglycerol (PG), phosphatidylcholine (PC), and PE (15, 16). Beranek *et al.* (17) and Ye *et al.* (18) have proposed models for CL remodeling in yeast. Like CL remodeling, PG remodeling has been reported in human mitochondria (19), but there is no report of it in yeast. Thus, the enzymes responsible for PG remodeling in yeast remain to be identified. Several studies have shown that CL is very important for mitochondrial function and growth on different carbon sources (17, 18). The growth defect is more pronounced at higher temperatures because CL is required to maintain the mitochondrial DNA and other important cellular functions (13). Defects in PE and CL metabolism cause mitochondrial dysfunction.

In this study, we report that Yor022c, a *Saccharomyces cerevisiae* mitochondrial protein (20) of the $iPLA_1$ family, is a novel mitochondrial phospholipase that hydrolyzes important mitochondrial phospholipids. Yor022c is a DDHD domain-

* This study was supported by the Council of Scientific and Industrial Research (CSIR), New Delhi, India under the 12th 5-year plan project (LIPIC). The authors declare that they have no conflicts of interest with the contents of this article.

[1] Supported by a fellowship from CSIR, New Delhi.

[2] Recipient of the J. C. Bose National Fellowship. To whom correspondence should be addressed: Central Food Technological Research Institute, Council of Scientific and Industrial Research, Mysore 570020, Karnataka, India. Tel.: 91-821-2517760; Fax: 91-821-2516308; E-mail: ram@cftri.com.

[3] The abbreviations used are: PA, phosphatidic acid; $iPLA_1$, intracellular phospholipase A_1; HSP, hereditary spastic paraplegia; PE, phosphatidylethanolamine; CL, cardiolipin; PG, phosphatidylglycerol; PC, phosphatidylcholine; NTA, nitrilotriacetic acid; MUG, more unsaturated group; LUG, less unsaturated group; PI, phosphatidylinositol; PS, phosphatidylserine; SM medium, synthetic minimal medium; MLCL, monolysocardiolipin; YPD, yeast extract-peptone-dextrose; Bistris propane, 1,3-bis[tris(hydroxymethyl)methylamino]propane; IP, immunoprecipitated; CIP, control immunoprecipitated.

containing serine hydrolase named Ddl1 (DDHD domain-containing lipase 1) that plays roles in CL, PE, and PG remodeling. We also suggest that Ddl1 has roles in CL degradation. In addition, we show that the *DDL1* gene is antagonistically regulated by Aft1 and Aft2 transcription factors.

Results

The DDL1 Gene and the Cellular Phospholipid Content—Ddl1 is a DDHD domain-containing protein that belongs to the $iPLA_1$ family of proteins. A list of homologs of the $iPLA_1$ family is available on the UniProtKB database. A sequence comparison was performed between selected members of the family that contained two conserved regions: the lipase motif (G*X*S*X*G) and the DDHD domain. An analysis of the sequences in the PROSITE database showed that the lipase motif is present inside the PROSITE domain PS00120 consensus sequence LIV-KG-LIVFY-LIVMST-G-HYWV-S-YAG-G-GSTAC, where the underlined amino acids are not accepted at a given position. In some family members, the lipase consensus sequence (G*X*S*X*G) was replaced by the S*X*S*X*G sequence. In Ddl1, the lipase motif spanned amino acids 499 to 503, whereas the DDHD domain spanned amino acids 519 to 700 (Fig. 1*A*).

As reported previously (1), DDHD domain-containing proteins play an important role in phospholipid metabolism. Therefore, we analyzed the phospholipid profiles of the *ddl1*Δ strain. The cells were grown in their respective media with 0.2 μCi of [^{14}C]acetate/ml. The lipids were extracted from stationary-phase cells and resolved on a silica-thin-layer chromatography (TLC) plate followed by phosphorimaging. The *ddl1*Δ strain did not show a significant change in the PA content compared with the wild-type strain (Fig. 1*B*). The deletion of the *DDL1* gene resulted in an increase (~21%) in the CL content in the cells, whereas the *ddl1*Δ strain did not show a substantial change in the content of other phospholipids (Fig. 1*C*). We also analyzed the phospholipid content of the important deletion strains in the CL metabolism (Fig. 1*C*). The *CLD1* gene encodes the known cardiolipin-specific phospholipase, whereas the *CRD1*gene encodes cardiolipin synthase. Gep4 is a phosphatase required for PG synthesis, and Taz1 is a transacylase required for CL remodeling. The CL-deficient and PG-rich *crd1*Δ strain was used as a negative control for CL and as a positive control for PG. The *gep4*Δ strain was used as a negative control for both CL and PG. The *crd1*Δ cells grown on glucose showed an accumulation of PG (1.79 ± 0.07% of the total phospholipids), which was confirmed using three different TLC solvent systems (solvent systems 1, 2, and 3). The cellular PA content did not change significantly upon overexpression of the *DDL1* gene (data not shown). Overexpression of the *DDL1* gene caused a significant decrease (~22%) in the cellular CL content on the *ddl1*Δ and (~33%) wild-type backgrounds compared with the vector control (Fig. 1*D*), whereas the PE content was elevated by ~16% on the *ddl1*Δ background and ~23% on the wild-type background (Fig. 1*E*). We also checked the effect of *DDL1* overexpression on the cellular content of the PG, an important intermediate of the CL biosynthesis. The cellular PG content did not change significantly upon overexpression of the *DDL1* gene on the *crd1*Δ background (data not shown). The TLC analyses of the deletion and overexpression studies suggested that the *DDL1* gene may have a potential role in the phospholipid metabolism.

Phospholipase Assay—To validate the role of the *DDL1* gene in phospholipid metabolism, we conducted a phospholipase activity assay using recombinant Ddl1 protein. Prior to the assays, the recombinant Ddl1 protein was purified from the yeast using nickel-nitrilotriacetic acid (Ni^{2+}-NTA) column chromatography and confirmed by immunoblotting with an anti-His_6 monoclonal antibody (Fig. 2*A*). All of the assays were conducted in the presence of the purified recombinant Ddl1 protein. The phospholipase assays with different fluorescently tagged phospholipids and native phospholipids showed that Ddl1 hydrolyzes CL, PE, and PG as substrates. Phospholipase activity was measured under different assay conditions. The protein-dependent (Fig. 2*B*) and time-dependent (Fig. 2*C*) lipase activity of Ddl1 was measured using fluorescently tagged CL, PE, and PG. The assays showed a protein- and time-dependent increase in the phospholipase activity. Similarly, pH-dependent and temperature-dependent assays were also conducted. Greater activity was observed at pH 8.5 and at 25 °C (data not shown).

The phospholipase activity of Ddl1 was measured using the native phospholipids (CL, PE, and PG) as substrates. The phospholipase activity of Ddl1 was higher for CL compared with PE and PG (Fig. 3*A*). PLA_1 activity toward the C18:1-, C18:0-, and C16:0-containing substrates (PE and PG) was not significantly different (Fig. 3*B*). Site-directed mutagenesis was conducted to evaluate the role of the G*X*S*X*G motif in lipase activity. The predicted amino acid residues Gly-499, Ser-501, and Gly-503 were replaced with alanine. The recombinant mutant Ddl1 proteins were purified from the yeast, similar to the wild-type Ddl1 protein. Mutations in the G*X*S*X*G motif (Gly to Ala) caused a significant reduction in the lipase activity of the protein, whereas the Ser to Ala mutation completely abolished the activity (Fig. 3*C*). Inoue *et al.* (4) have suggested that the DDHD domain is crucial for the PLA_1 activity. Therefore, to check the effect of the DDHD domain on the phospholipase activity of the Ddl1, we created a DDHD domain deletion protein (truncated Ddl1). Like wild-type Ddl1, the truncated Ddl1 protein was purified, and the phospholipase activity assays were performed. The data indicated that the DDHD domain deletion significantly reduced the phospholipase activity of the Ddl1 (Fig. 3*D*). Collectively, these experiments suggested that Ddl1 is a novel phospholipase that uses key mitochondrial membrane lipids as substrates.

DDL1 Alters the Molecular Species Profile of CL, PE, and PG—Phospholipase assays revealed that Ddl1 hydrolyzes CL, PE, and PG. Therefore we checked the effect of the Ddl1 on molecular species of its substrates using the MS/MS^{ALL} technique. An analysis of the molecular species of CL revealed that the C64 to C68 clusters harbored the majority of the CL species, as reported previously (21). The major CL molecular species clusters (CL C64 to C68) were grouped into two groups, the more unsaturated group (MUG) and the less unsaturated group (LUG). The deletion of the *DDL1* gene significantly altered the profile of the CL species (Fig. 4*A*). In the *ddl1*Δ strain, the CL species with saturated fatty acids (LUG) were increased at the expense of the CL species with unsaturated fatty acids (MUG).

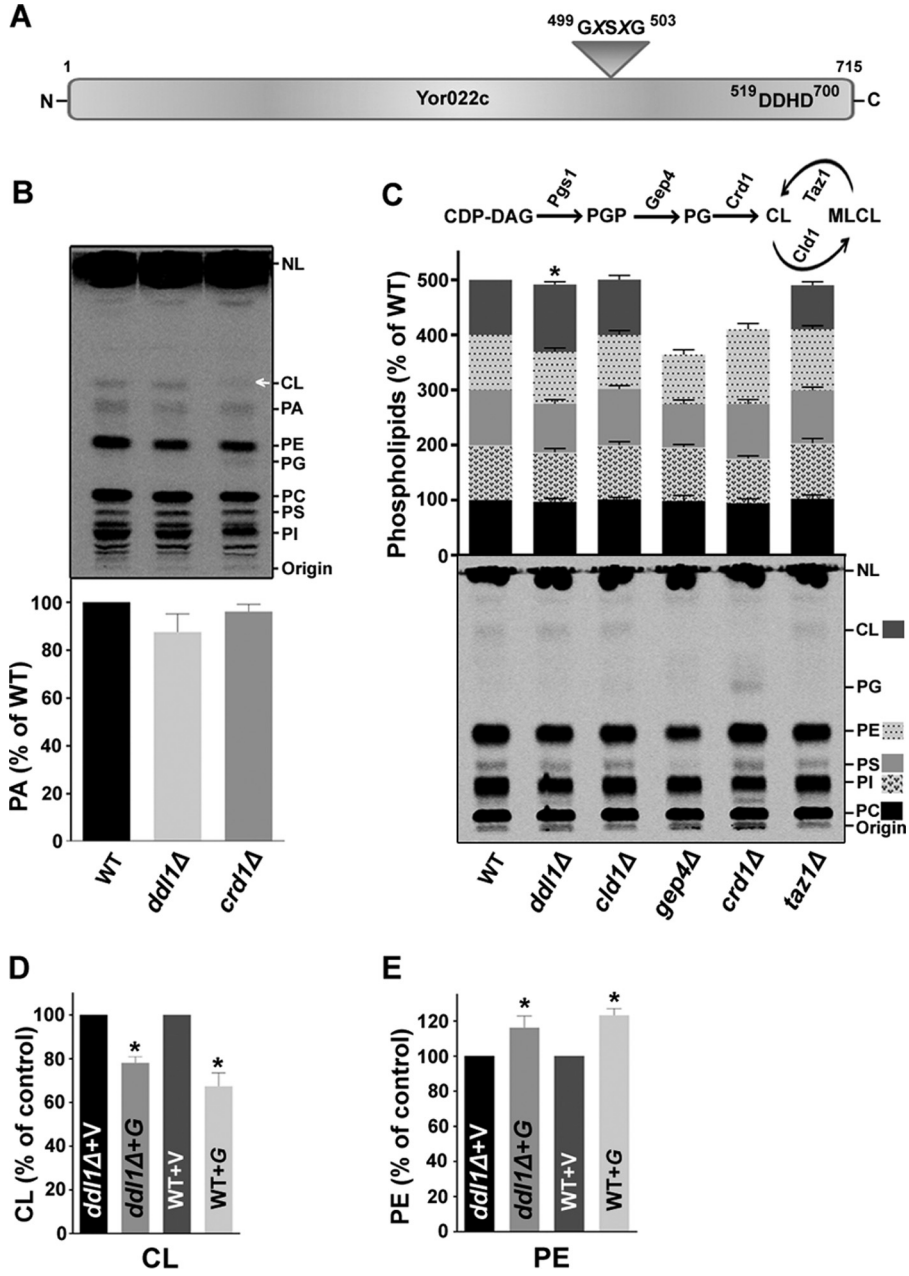

FIGURE 1. **Effect of the *DDL1* gene on the cellular phospholipid content.** *A*, schematic diagram representing the two conserved regions: the lipase motif and DDHD domain in the Ddl1 (Yor022c) protein. *B* and *C*, effect of deletion of the *DDL1* gene on phospholipids content. In *B*, an unidentified lipid species also migrated at the position of CL in the *crd1*Δ strain (indicated by an *arrow*). *NL*, nonpolar lipids. In *C*, a schematic diagram represents the key enzymes of CL metabolism (*upper panel*), and the extracted lipids were analyzed on a TLC plate (*bottom panel*). *D* and *E*, *DDL1* overexpression and cellular CL and PE levels. *V*, pYES2/NT B vector; *G*, pYES2/NT B-*DDL1*. In each TLC analysis, the lipids that were extracted from the stationary-phase cells ($A_{600} = 25$) grown in the presence of [^{14}C]acetate were analyzed on a TLC plate followed by phosphorimaging, and the label was counted with a liquid scintillation counter. To show each phospholipid, the optimum brightness and contrast were adjusted in the images. The values are presented as the mean ± S.E. ($n = 3$). Significance was determined at *, $p < 0.05$.

We also analyzed the CL species of *cld1*Δ and *taz1*Δ strains because the *CLD1* and *TAZ1* genes play an important role in CL remodeling (Fig. 4*A*). *DDL1* overexpression did not significantly affect the molecular species of CL in the *cld1*Δ strain, but it caused an increase in the CL species with unsaturated fatty acids (MUG) at the expense of the CL species with saturated fatty acids (LUG) on the *ddl1*Δ background (Fig. 4*B*). In contrast, *DDL1* overexpression on the wild-type background increased the CL species with saturated fatty acids (LUG) at the expense of the CL species with unsaturated fatty acids (Fig. 4*B*). A comparison of the *ddl1*Δ, and wild-type strains showed that there was a relative increase in the C32:0 and a decrease in the C32:1 species of PE (Fig. 4*C*). An analysis of *DDL1* overexpression on the *ddl1*Δ background showed that there was an increase in the C34:2 species of PE (Fig. 4*D*). *DDL1* overexpression on the *crd1*Δ background caused a significant increase in the C34:2 and C34:1 species of PG at the expense of the C32:1 and C32:0 species (Fig. 4*E*).

We also analyzed the effect of the *DDL1* gene on the molecular species of other phospholipids. The analysis showed that

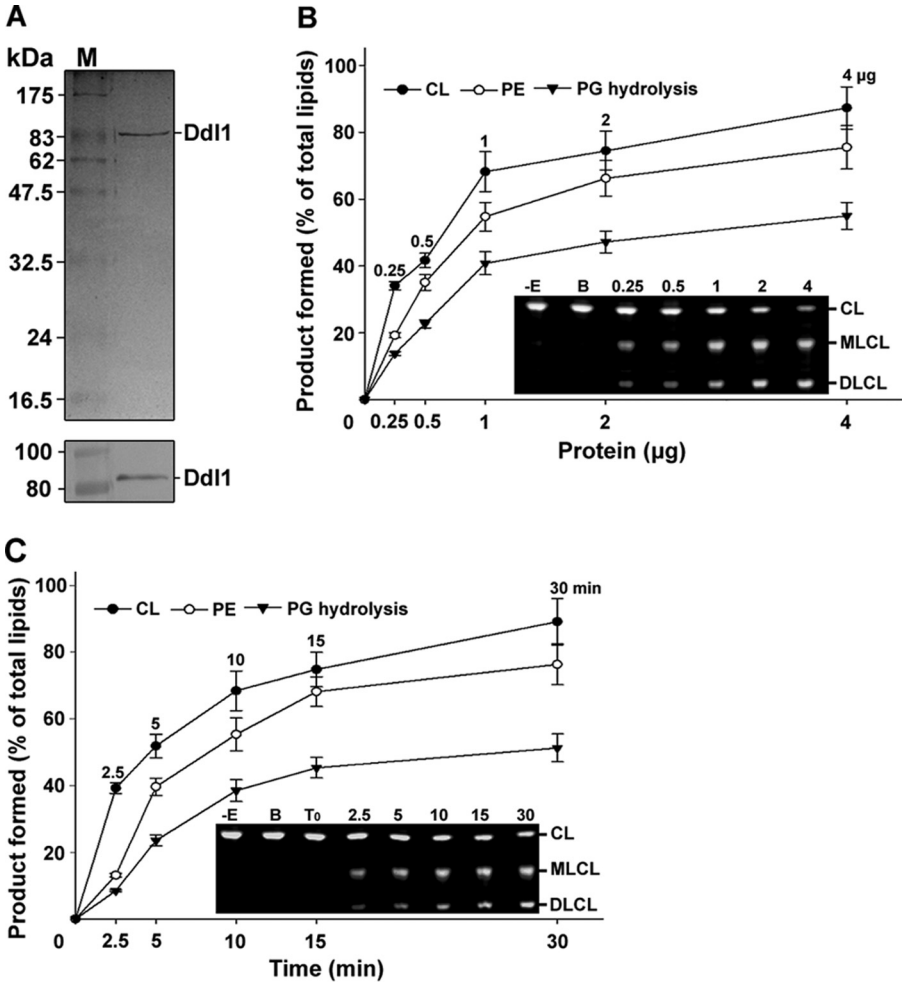

FIGURE 2. **Purification and biochemical function of the Ddl1 protein.** *A*, purification of the recombinant protein. *Upper panel*, the purified recombinant yeast Ddl1 protein was resolved by 12% SDS-PAGE and stained with Coomassie Brilliant Blue. *Lower panel*, immunoblot analysis of the Ddl1 protein with an anti-His_6 monoclonal antibody (*M*, protein marker). *B*, protein-dependent assay. Fluorescently tagged CL, PE, and PG were hydrolyzed with an increasing amount of the purified protein for 10 min at 30 °C (−*E*, without enzyme; *B*, boiled enzyme). *C*, time-dependent assay. The fluorescently tagged phospholipids were hydrolyzed in the presence of 1 μg of the purified protein at 30 °C at different time intervals. T_0, zero time point (the enzyme was added to the reaction mixture, which was immediately stopped). The assay was conducted in the presence of 5 μM fluorescently labeled substrate. The reaction was stopped, and the lipids were resolved on a TLC plate and quantified with GeneTools software. A portion of the representative TLC plate is shown. The values are presented as the mean ± S.E. ($n = 3$).

like with PE and PG, the C32 and C34 clusters harbored the majority of the PA, PC, phosphatidylinositol (PI), and phosphatidylserine (PS), species, as reported previously (22). The comparative analysis showed that the *DDL1* deletion and overexpression altered the molecular species profile of PA and PS (Fig. 5, *A*–*D*). In the *ddl1*Δ strain, the molecular species of PC and PI were altered, but *DDL1* overexpression did not change the molecular species of these phospholipids (Fig. 5, *E*–*H*). These changes could be due to the indirect effect of the *DDL1* gene, as Ddl1 did not show lipase activity toward these phospholipids. Together, the phospholipase assays and the phospholipids analyses of the deletion and overexpression studies suggested that the *DDL1* gene may have a potential role in the CL metabolism.

AFT1 and AFT2 Antagonistically Regulate the DDL1 Gene—To identify the transcription factor that putatively binds the upstream promoter region of the *DDL1* gene, we searched the Yeastract promoter database of *S. cerevisiae*, which provided us with 23 different transcription factors. However, none of them are directly involved in the regulation of mitochondrial functions. Recently, Berthelet *et al.* (23) have shown that the *AFT1* gene has iron-independent functions and affects mitochondrial function. Therefore, we selected Aft1 and its paralog, Aft2, both of which bind at the same sequence (Fig. 6*A*). First, we examined the expression of the *DDL1* gene on the *aft1*Δ and *aft2*Δ backgrounds. The *AFT1* deletion caused an increase in the expression of the *DDL1* transcripts, whereas the *AFT2* deletion caused a decrease in the level of the *DDL1* transcripts. *AFT2* was up-regulated (8.87-fold) in the *aft1*Δ strain, and *AFT1* was up-regulated 7.46-fold in the *aft2*Δ strain (Fig. 6*B*). Compared with the vector control, *AFT1* overexpression caused a slight down-regulation of the *DDL1* transcripts, whereas *AFT2* overexpression up-regulated (~12-fold) the expression of the *DDL1* gene (Fig. 6*C*). To assess the transcriptional regulation of the *DDL1* gene by Aft1/2 *in vivo*, the β-galactosidase activity of *DDL1-lacZ* was measured in the WT, *aft1*Δ, and *aft2*Δ strains. The β-galactosidase activity of the *aft1*Δ strain was significantly higher (~37%), and that of the *aft2*Δ strain was lower (~52%)

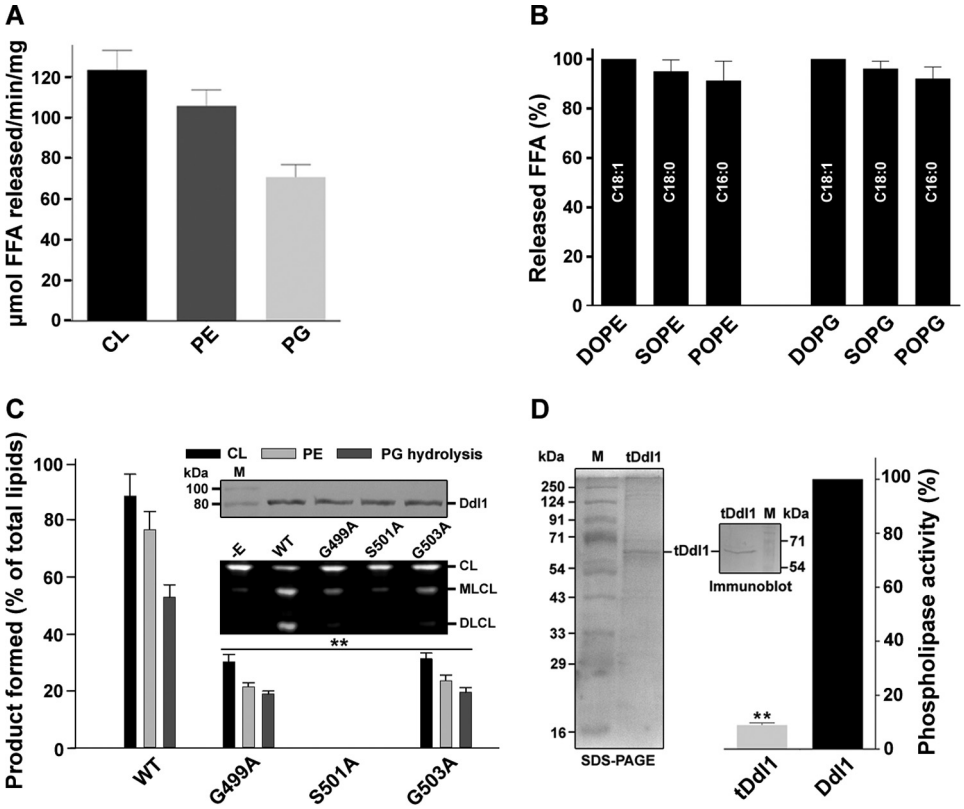

FIGURE 3. **Characterization of the *DDL1* gene.** *A*, phospholipase assay and measurement of the released FFA. The assays were conducted using the purified recombinant Ddl1 protein. The released FFA, estimated using a fluorescent FFA estimation kit, are represented as μmol of FFA released/min/mg of protein. *B*, phospholipase assay using PE and PG with different fatty acid compositions. The assay was conducted for 30 min at 30 °C in the presence of 2 μg of the purified recombinant Ddl1 and 100 μM substrates. The released FFA were scraped from the TLC plates, and the samples were prepared and subjected to gas chromatography analysis: DOPE, 18:1–18:1 PE; SOPE, 18:0–18:1 PE; POPE, 16:0–18:1 PE; DOPG, 18:1–18:1 PG; SOPG, 18:0–18:1 PG; POPE, 16:0–18:1 PG. *C*, site-directed mutagenesis of the lipase motif and phospholipase activity. *Upper insert*, the recombinant Ddl1 mutant proteins were purified from yeast similar to the wild-type Ddl1 protein, and an immunoblot analysis was performed. *Lower insert*, 1 μg of the purified wild-type and mutant Ddl1 proteins was used for the phospholipase assay at 30 °C for 30 min. A portion of the representative TLC plate is shown. *D*, effect of the DDHD domain on the phospholipase activity of Ddl1. The purified recombinant truncated Ddl1(tDdl1) protein (*left panel*) and an immunoblot of the tDdl1 (*middle panel*) are shown. *Right panel*, 1 μg of the purified wild-type and tDdl1 proteins was used for the phospholipase assay at 30 °C for 30 min. The reaction was stopped, and the lipids were resolved on a TLC plate and quantified with GeneTools software. *M*, protein marker; $-E$, without enzyme; *WT*, pYES2/NT B-*DDL1*. The values are presented as the mean ± S.E. ($n = 3$), and significance was determined at **, $p < 0.01$.

than the wild-type strain (Fig. 6*D*). These results suggested that Aft1 negatively regulates *DDL1* expression, whereas Aft2 positively regulates its expression.

It has been shown that Aft1 and Aft2 bind a conserved iron-responsive element (Fe-RE) site present in the promoters of their gene targets. Fe-RE binding sites consist of a CACCC core sequence (24). Chromatin immunoprecipitation (ChIP) assays were performed to assess the *in vivo* binding of Aft1/2 to the *DDL1* promoter. The ChIP assays revealed that both Aft1 and Aft2 occupy the *DDL1* promoter (Fig. 6*E*). To confirm the binding of Aft1/2 to the *DDL1* promoter, gel shift assays were performed using the bacterially expressed and purified recombinant Aft1/2 proteins. The proteins were purified by Ni^{2+}-NTA column chromatography. We were able to purify Aft2 protein, but the Aft1 protein was only partially purified (Fig. 7*A*). As the amount of protein increased, a decrease in the free DNA and an increase in the formation of the DNA-protein complex were observed (Fig. 7, *B* and *C*). Electrophoretic mobility shift assays (EMSAs) conducted in the presence of an anti-His_6 monoclonal antibody (Ab) showed stronger DNA-protein complex formation. Fe^{2+} prevented Aft1/2 binding (Fig. 7*D*). Together, the data from the expression analysis, β-galactosidase activity assays, ChIP assays, and gel shift assays suggested that Aft1 and Aft2 antagonistically regulate *DDL1* gene.

Knock-out and Overexpression of the DDL1 Gene Produce Mitochondrial Dysfunction—It was reported previously that the Ddl1 protein is localized in the mitochondria (20), and we showed that it acts as a phospholipase that hydrolyzes the major mitochondrial phospholipids species. Therefore, we investigated the effect of the *DDL1* gene on the mitochondria in the cells. Cells grown in stationary phase in synthetic minimal (SM) medium were collected and stained with the mitochondrial dye MitoTracker Orange CMTMRos followed by confocal microscopy. Microscopic imaging showed that alterations in CL metabolism produce mitochondrial dysfunction. The *ddl1*Δ strain showed a significant increase (69.46%) in fragmented mitochondria compared with the wild-type cells (24.87%). A similarly significant pattern was also observed in the other deletion strains in CL metabolism (Fig. 8*A*). Ye *et al.* (18) have shown that the deletion of *CLD1* (the only known CL-specific phospholipase A_2 in *S. cerevisiae*) on the *taz1*Δ background rescues the respiration defect of the mutant. Therefore, we also investigated the effect of the *DDL1* and *CLD1* deletions on the mitochondria in the *taz1*Δ strain. *CLD1* deletion in the *taz1*Δ

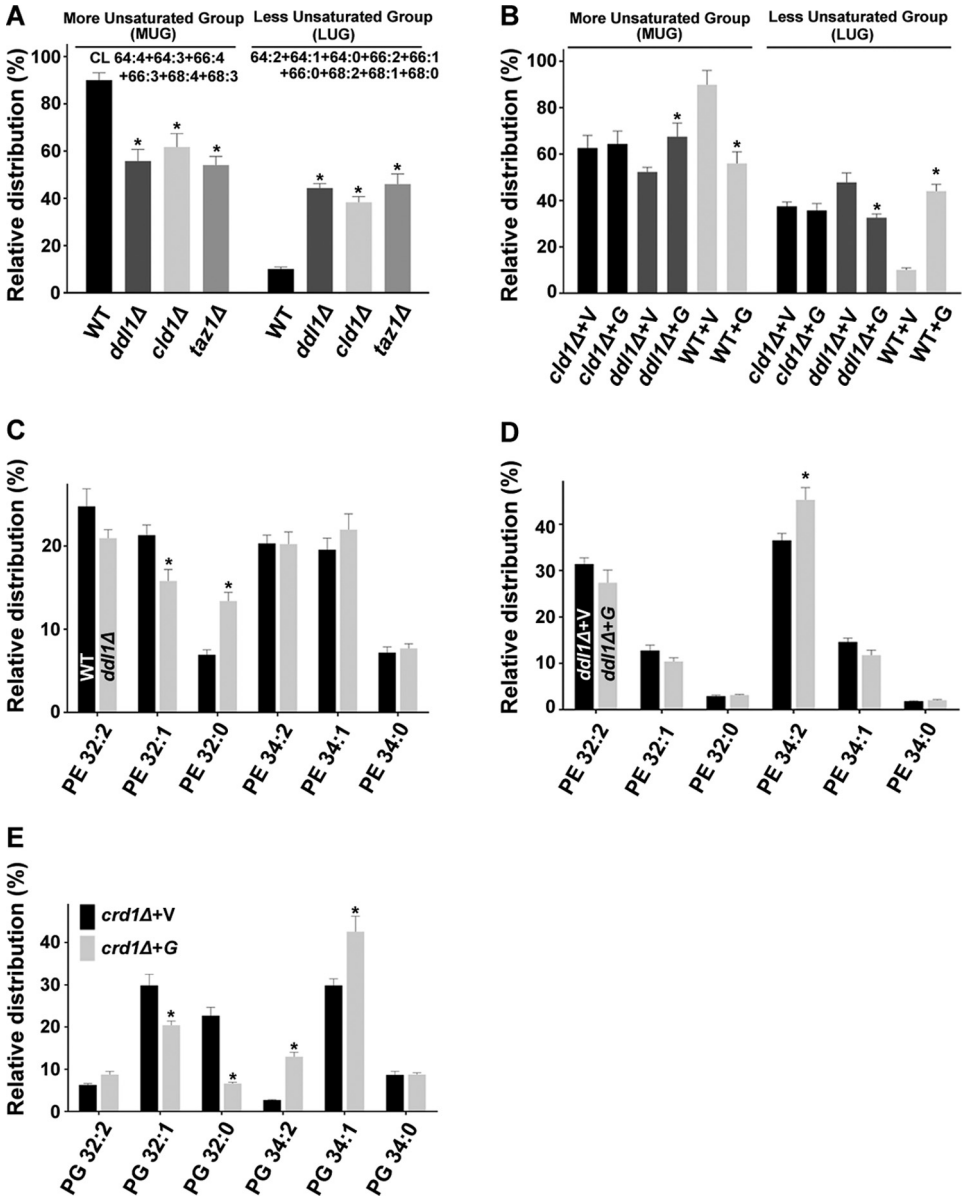

FIGURE 4. **Effect of the *DDL1* gene on the molecular species of CL, PE, and PG.** *A–E*, effect of the *DDL1* gene on the molecular species of CL (*A* and *B*), PE (*C* and *D*), and PG (*E*). In each case, the extracted lipids were analyzed by MS/MS^{ALL}. For the relative quantification of CL, a graph was generated for the *MUG* and the *LUG* of each strain, and for PE and PG, the amount of each molecular species was determined relative to the total species present in both clusters (C32 and C34). *V*, pYES2/NT B vector; *G*, pYES2/NT B-*DDL1*. The values are presented as the mean ± S.E. ($n = 3$). Significance was determined at *, $p < 0.05$.

strain showed a significant reduction in the mitochondrial fragmentation pattern (53.93%) in comparison with the *taz1*Δ strain (79.65%), whereas the *DDL1* deletion in the *taz1*Δ strain caused an increase (93.36%) in the fragmentation pattern (Fig. 8*A*). To understand the effects of CL-hydrolyzing phospholipases on mitochondrial function, we generated a triple deletion strain (*RRY25*, *cld1*Δ*ddl1*Δ*taz1*Δ) on the *taz1*Δ background. Interestingly, compared with the *taz1*Δ strain (79.65%), the triple mutant showed reduced (40.44%) mitochondrial fragmentation (Fig. 8*A*).

DDL1 overexpression caused an increase (~14% on the *ddl1*Δ background and ~30% on the wild-type background) in the number of cells with fragmented mitochondria (Fig. 8*B*). The effect of *DDL1* overexpression on the mitochondrial inner membrane potential was investigated with potentiometric JC-1 dye (5,5′,6,6′-tetrachloro-1,1′,3,3′tetraethylbenzimidazolylcarbocyanine iodide). *DDL1* overexpression caused a reduction (~21% on the *ddl1*Δ background and ~23% on the wild-type background) in the mitochondrial inner membrane potential of the cells (Fig. 8*C*). *DDL1* overexpression caused a substantial reduction in the rate of oxygen consumption in the cells (Fig. 8*D*).

We also examined the CL content in the double and triple mutants. Compared with the *taz1*Δ strain, the TLC analysis showed a substantial increase (~51%) in the CL content of the triple mutant, whereas the CL contents of the *ddl1*Δ*taz1*Δ and *cld1*Δ*taz1*Δ strains were not significantly different (Fig. 9*A*). We also checked the molecular species profile of CL in the *cld1*Δ*ddl1*Δ*taz1*Δ strain, which showed no significant difference (Fig. 9*B*). The TLC data showed that compared with the

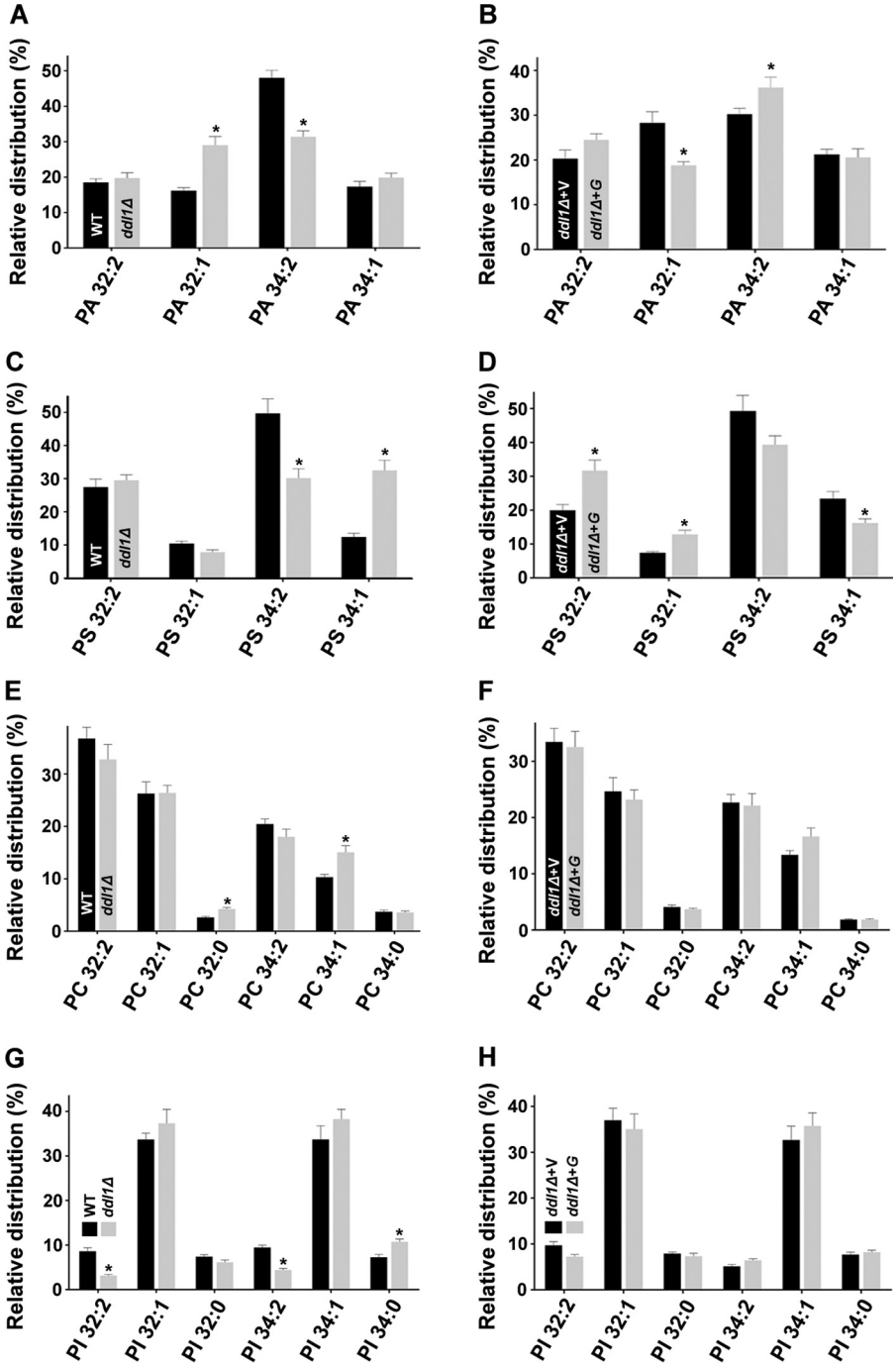

FIGURE 5. **Effect of the *DDL1* gene on the molecular species of the different phospholipids.** *A–H*, effect of the *DDL1* gene on the molecular species of the different phospholipids: PA (*A* and *B*), PS (*C* and *D*), PC (*E* and *F*), and PI (*G* and *H*). In each case, the extracted lipids were analyzed by MS/MS^{ALL}. For the relative quantification of the phospholipids, the amount of each molecular species was determined relative to the total species present in both clusters (C32 and C34). *V*, pYES2/NT B vector; *G*, pYES2/NT B-*DDL1*. The values are presented as the mean ± S.E. ($n = 3$). Significance was determined at *, $p < 0.05$.

*taz1*Δ strain, the *cld1*Δ*ddl1*Δ*taz1*Δ strain exhibited reduced monolysocardiolipin (MLCL) content (Fig. 9*C*). The *ddl1*Δ and *cld1*Δ*ddl1*Δ strains also showed a faintly detectable amount of MLCL, but MLCL was absent in the *cld1*Δ strain (data not shown). We also performed an expression analysis of the *DDL1* and *CLD1* genes on the *taz1*Δ background, which showed that the expression of these genes was increased (~6-fold) (Fig. 9*D*). Briefly, these experiments suggested that both the deletion and overexpression of the *DDL1* gene produce mitochondrial dysfunction and that the *DDL1* gene plays an important role in the CL metabolism.

AFT1/2-defective Strains Exhibit Altered CL Metabolism and Mitochondrial Dysfunction—As reported previously, the *AFT1* gene affects mitochondrial function; therefore, we investigated the effects of the *AFT1/2* genes on the signature phospholipid species (CL) of the mitochondria. The cells were grown in their respective media with 0.2 μCi of [^{14}C]acetate/ml. The lipids that were extracted from the stationary-phase

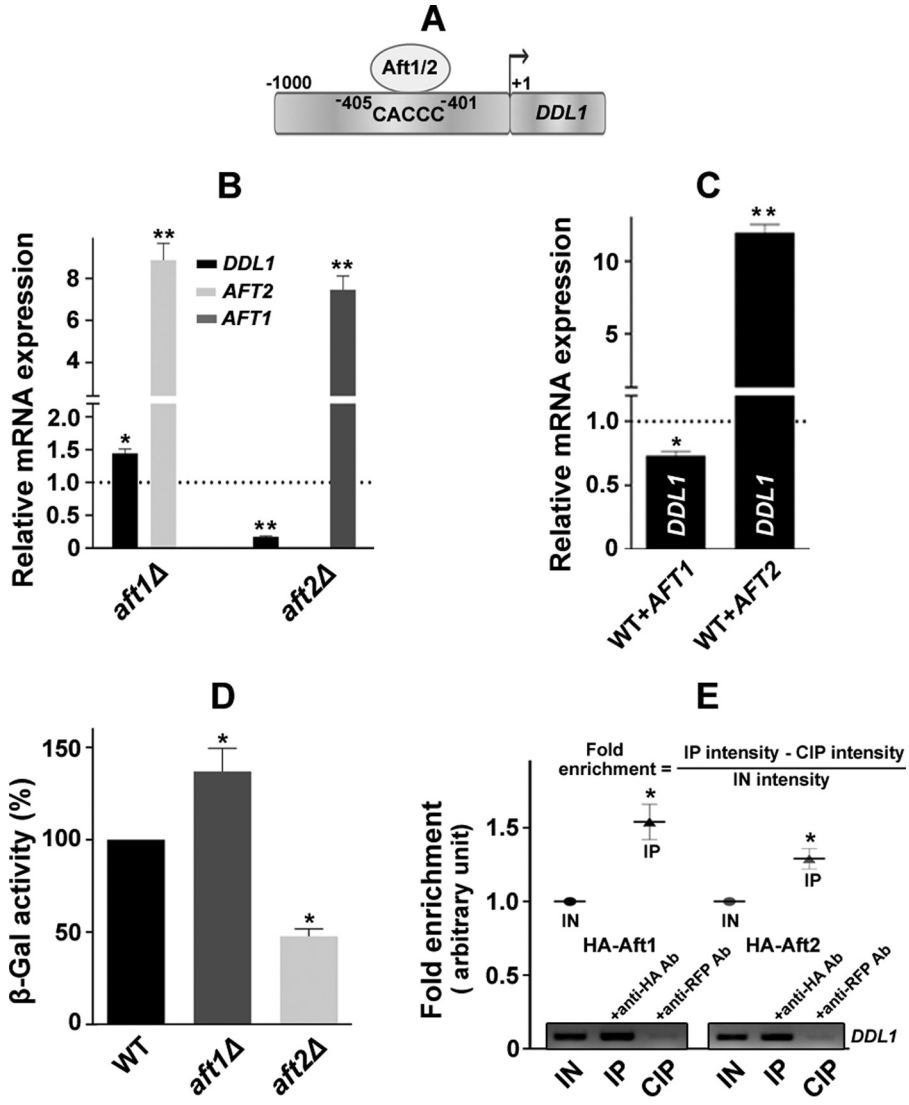

FIGURE 6. **Regulation of the *DDL1* gene by the *AFT1* and *AFT2* transcription factors.** *A*, schematic diagram of the *DDL1* promoter representing the Aft1/2 binding site and sequence. *B* and *C*, effect of the *AFT1* and *AFT2* genes on the expression of the *DDL1* gene. The *horizontal dotted lines* represent expression in the WT/vector control strain. The values are presented as the mean ± S.E. ($n = 3$) and are represented as fold changes. Significance was determined at *, $p < 0.05$; and **, $p < 0.01$. *D*, β-galactosidase activity of *DDL1-lacZ* in the *aft1*Δ and *aft2*Δ strains. The *graph* shows β-galactosidase activity under the control of the *DDL1* promoter in the WT, *aft1*Δ, and *aft2*Δ strains, represented as a % of the WT. The values are presented as the mean ± S.E. ($n = 3$). *E*, association of Aft1 and Aft2 with the *DDL1* promoter. Transformants (BG1805-*AFT1/2*) overexpressing the Aft1/2 proteins were subjected to ChIP assays with anti-HA and anti-RFP antibodies. PCR analyses of the input (*IN*), IP, and CIP DNA using the *DDL1* promoter-specific primers show the occupancy of Aft1/2 on the *DDL1* promoter. The relative fold enrichment was measured using the formula shown at the *top*. The values are presented as the mean ± S.E. ($n = 3$) and represent the fold enrichment (arbitrary unit). Significance was determined at *, $p < 0.05$.

cells were resolved on a TLC plate followed by phosphorimaging. The *aft1*Δ strain showed a decrease (~16%) in CL content of the cells compared with the wild-type strain, whereas deletion of the *AFT2* gene caused an increase (~17%) in the CL content (Fig. 10*A*). Overexpression of the *AFT1* gene on the *aft1*Δ background caused an increase (~22%) in the CL content, but *AFT1* overexpression on the wild-type background caused a decrease in the CL content. The cellular CL content was significantly decreased upon *AFT2* overexpression (Fig. 10*B*).

Deletions of the *AFT1/2* genes altered the CL species profile. In the *aft1*Δ strain, the CL species with saturated fatty acids (LUG) were increased, and this change was more profound in the *aft2*Δ strain (Fig. 10*C*). An analysis of *AFT1* overexpression on the *aft1*Δ background did not complement the CL molecular profile; in addition, it exacerbated the condition by increasing the CL species with saturated fatty acids (LUG). *AFT2* overexpression on the *aft2*Δ background increased the CL species with unsaturated fatty acids (MUG). *AFT1/2* overexpression on the wild-type background did not affect the CL molecular profile (Fig. 10*D*).

To assess the role of the *AFT1/2* genes on the mitochondria, we stained the stationary-phase cells grown in SM medium with the mitochondrial dye MitoTracker Orange CMTMRos followed by confocal microscopy. Microscopic imaging revealed that the deletion of *AFT1* produced a significant increase (66.8%) in the number of cells with fragmented mitochondria compared with the wild-type strain (24.87%). *AFT2* deletion also increased the mitochondrial fragmentation (Fig. 11*A*).

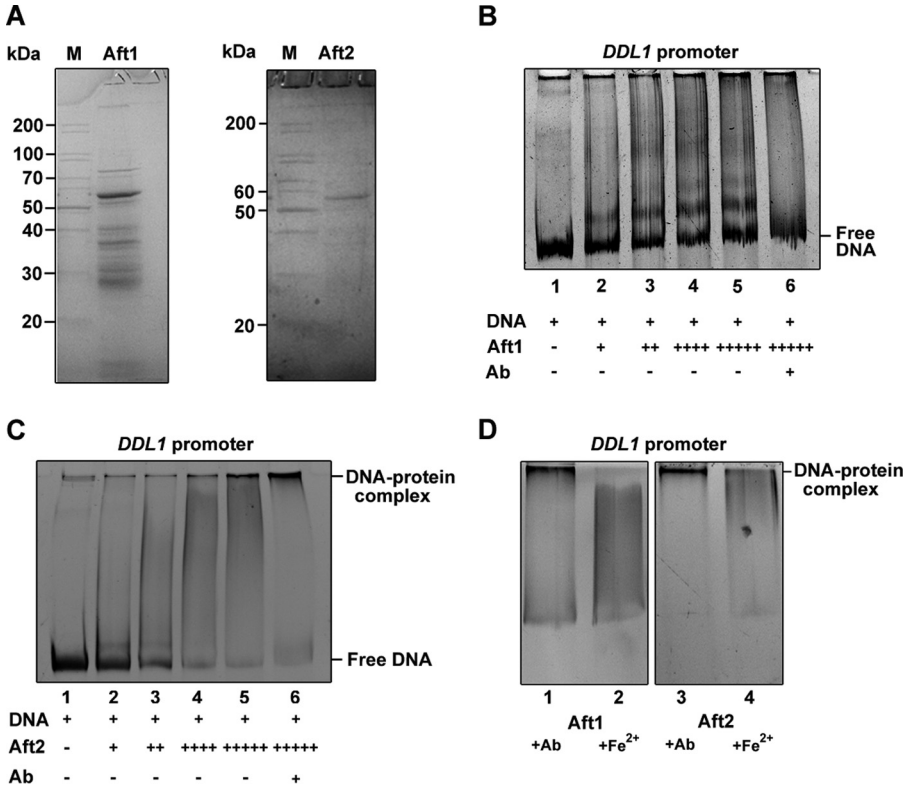

FIGURE 7. **EMSAs.** *A*, Aft1 and Aft2 proteins were expressed in pRSET A in bacteria, purified, resolved by 12% SDS-PAGE, and stained with Coomassie Brilliant Blue. *Left panel*, *lane 1*, protein marker (*M*); *lane 2*, Aft1 protein. *Right panel*, *lane 1*, protein marker; *lane 2*, Aft2 protein. *B* and *C*, EMSAs of Aft1/2 on the *DDL1* promoter. *Lane 1*, *DDL1* promoter DNA alone (200 ng). The protein-dependent EMSA study is shown with increasing amounts of purified Aft1 and Aft2 proteins (200 ng to 1 μg, *lanes 2–5*) in the presence of 200 ng of the *DDL1* promoter DNA (1 kb). In each assay, one reaction was performed in the presence of a monoclonal anti-His_6 Ab (*lane 6*). *D*, EMSA with the purified Aft1/2 proteins (1 μg) in the presence of 200 ng of promoter DNA (1 kb) of *DDL1* and Ab (*lane 1* and *3*) or Fe^{2+} (*lane 2* and *4*). Data are representative, and the experiment was repeated three times.

AFT1 overexpression on the *aft1*Δ background did not significantly improve the dysfunction in the mitochondria. *AFT1* overexpression on the wild-type background caused an increase (~38%) in the number of cells with fragmented mitochondria (Fig. 11*B*). *AFT2* overexpression caused an increase in the number of cells with fragmented mitochondria (~20% on the *aft2*Δ background and ~50% on the wild-type background) (Fig. 11*B*). Together, the mass spectrometry, TLC analyses, and microscopic imaging of the deletion and overexpression strains suggested that *AFT1/2* play a role in CL metabolism and that the *AFT1/2*-defective strains produce mitochondrial dysfunction.

Discussion

Ddl1 is the serine hydrolase of the $iPLA_1$ family. Phospholipase assays and site-directed mutagenesis revealed that Ddl1 is a novel mitochondrial phospholipase that hydrolyzes key mitochondrial phospholipids. Although it is likely a PA-PLA_1, Ddl1 did not show lipase activity toward PA. Deletion of the *DDL1* gene caused an increase in the CL content. This could be due to the deletion of CL-preferring lipase leading to CL accumulation. Compared with the vector control, the overexpression of the *DDL1* gene on any genetic background caused a significant decrease in the cellular CL content and an increase in the PE content. The increased PE content upon *DDL1* overexpression could be due to CL deficiency; Gohil *et al.* (14) have suggested that CL and mitochondrial PE have overlapping functions and that each can compensate for the loss of the other. Interestingly, the *crd1*Δ cells grown on glucose accumulated PG (~1.8% of the total phospholipids), likely because the expression of the CL biosynthetic genes is up-regulated in stationary-phase cells (18).

In mammals, it is well established that CL remodeling can be achieved via two pathways, similar to the remodeling of other phospholipids. The first occurs via the Lands cycle, a deacylation-reacylation cycle (CoA-dependent) and the second occurs via a deacylation-transacylation cycle (CoA-independent) between acceptor and donor phospholipids. Several models based on the deacylation-transacylation cycle have been proposed for CL remodeling in yeast. Barth syndrome patients have been shown to be defective in CL and PG remodeling (15). PG undergoes remodeling in human mitochondria to achieve appropriate fatty acyl chains and to prevent the harmful effects of LPG accumulation (19). Unlike in human, there is no report on PG remodeling in yeast. Recently, Pokorna *et al.* (25) have reported the presence of two diverse pools of PG with different fatty acid compositions in yeast mitochondria. Like lysophosphatidylglycerol (LPG), the accumulation of Lysophosphatidylethanolamine (LPE) may cause adverse effects to the cells. Therefore, considering these facts, it can be hypothesized that Ddl1 may play an important role in the remodeling of CL, PE, and PG (as Ddl1 hydrolyzes these substrates).

Deletion of the *DDL1* gene caused an increase in the saturated species of CL and PE, whereas overexpression of the

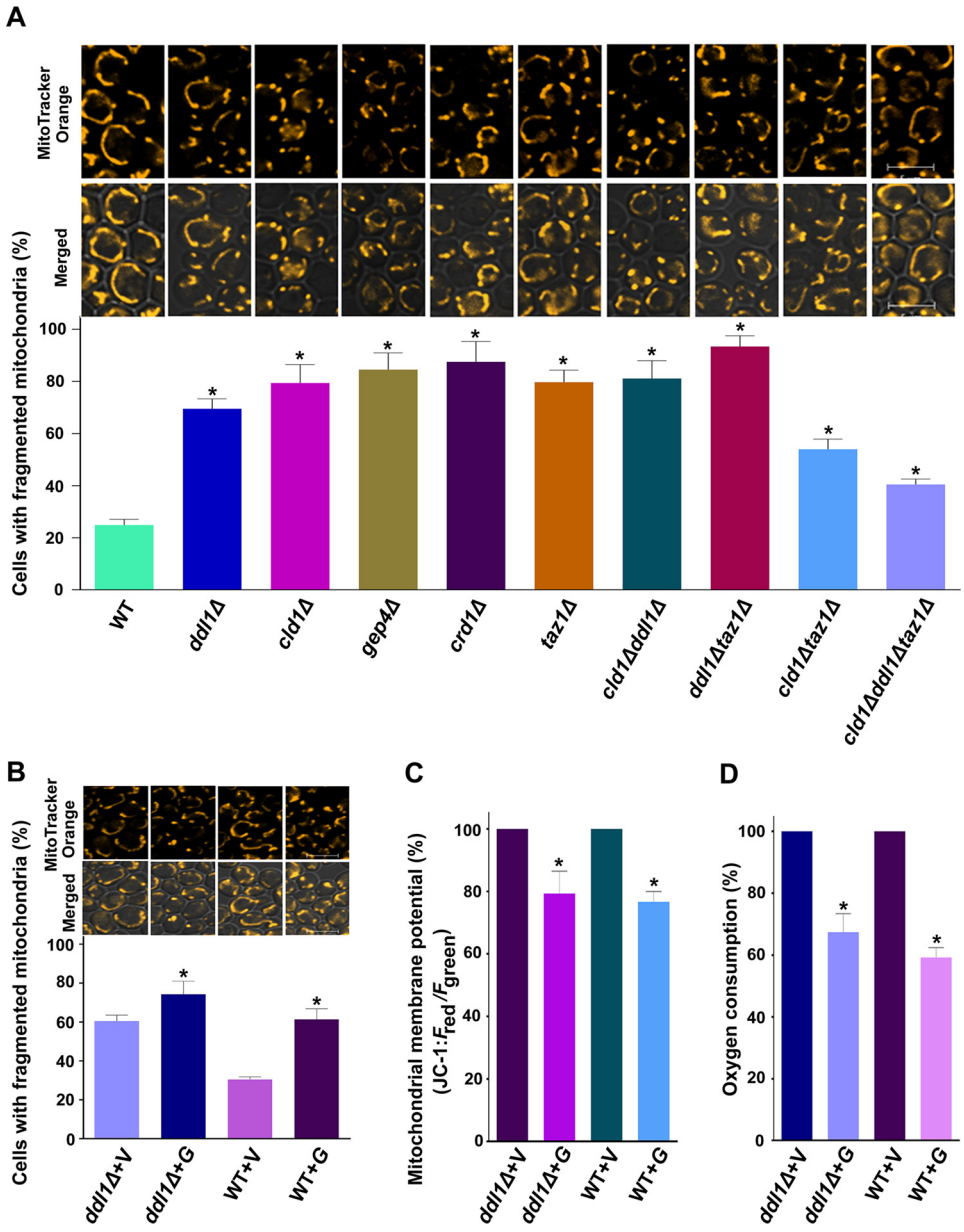

FIGURE 8. **Physiological significance of the *DDL1* gene.** *A* and *B*, the role of the *DDL1* gene in mitochondrial morphology. Stationary-phase cells were stained with the mitochondrial dye MitoTracker Orange CMTMRos. The images were captured with a confocal microscope. *C*, study of the mitochondrial membrane potential. The cells were collected from the stationary phase and stained with the JC-1 dye. The ratio of F_{red}/F_{green} was used to determine the relative mitochondrial membrane potential. *D*, *DDL1* overexpression and the oxygen consumption rate. The cells were collected from the stationary phase, and the oxygen consumption rate was analyzed. *Bar*, 5 μm. *V*, pYES2/NT B vector; *G*, pYES2/NT B-*DDL1*. To quantify mitochondrial fragmentation, at least 200 cells were scored in each background. The values are presented as the mean ± S.E. ($n = 3$). Significance was determined at *, $p < 0.05$.

DDL1 gene increased the unsaturated species. Interestingly, *DDL1* overexpression did not significantly affect the molecular species of CL in the *cld1*Δ strain, which indicates that Ddl1 acts independently. *DDL1* overexpression on the *crd1*Δ background caused a significant increase in the unsaturated species of PG. Considering these results, we propose that CL is remodeled through a deacylation-transacylation cycle in which MLCL is generated from CL by phospholipases (Cld1 and Ddl1) followed by MLCL reacylation by transacylase (Taz1). Thus, the acyl specificity of CL is achieved by extensive remodeling through PLA_1 (Ddl1), PLA_2 (Cld1), and transacylase (Taz1) activities. In addition, we also propose a role for Ddl1 in CL degradation (Fig. 12). The dilysocardiolipin formed by Ddl1 activity initiates CL degradation (26). We propose that a deacylation (by Ddl1)-reacylation (by CoA-dependent acyltransferase) cycle is responsible for PE and PG remodeling in yeast. With its broad substrate specificity, the Ale1 (also known as Lpt1) protein may reacylate the LPE and LPG generated by Ddl1 activity to PE and PG, respectively (27, 28). It will be interesting to study the relationship between the *DDL1* and *ALE1* genes in phospholipid metabolism.

It has been shown that CL is very important for the mitochondrial functions. The *taz1*Δ strain displayed a low CL content and no accumulation of PG, suggesting that the PG to CL biosynthesis is not affected in the *taz1*Δ strain. However, the reduced CL content indicated that CL hydrolysis/degradation

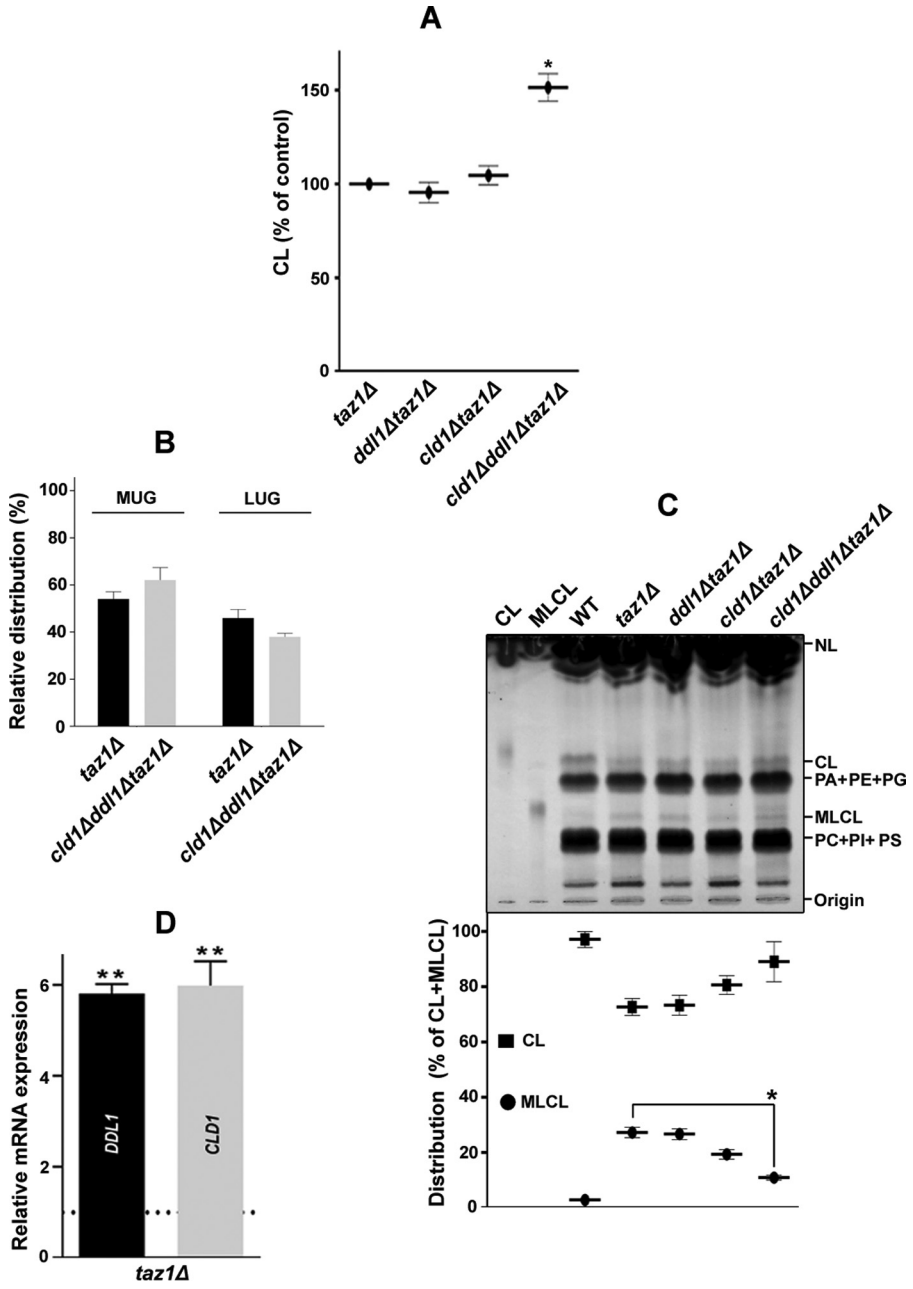

FIGURE 9. **The *DDL1* gene and cellular MLCL content.** *A*, effects of the *TAZ1*, *DDL1*, and *CLD1* genes on the cellular CL content. The lipids that were extracted from the stationary-phase cells ($A_{600} = 25$) grown in the presence of [^{14}C]acetate were analyzed on a TLC plate. *B*, *TAZ1*, *DDL1*, and *CLD1* genes and molecular species of CL. The molecular species of CL in the *cld1*Δ*ddl1*Δ*taz1*Δ strain were compared with the *taz1*Δ control, and the data for the *taz1*Δ strain were duplicated from Fig. 4*A*. *C*, effects of the *TAZ1*, *DDL1*, and *CLD1* genes on the cellular MLCL content. The lipids that were extracted from the stationary-phase lyophilized cells (50 mg) were resolved on a TLC plate, which was then charred with 10% cupric sulfate in 8% aqueous phosphoric acid for 10 min at 180 °C. The amounts of CL and MLCL were determined relative to the total CL (CL + MLCL). *D*, analysis of the expression of the *DDL1* and *CLD1* genes in the *taz1*Δ strain. The *horizontal dotted line* represents expression in the WT strain. The values are represented as fold changes. The values are presented as the mean ± S.E. ($n = 3$), and significance was determined at *, $p < 0.05$; and **, $p < 0.01$.

may have increased. An analysis of the expression of the *DDL1* and *CLD1* genes on the *taz1*Δ background showed a significant increase in their expression levels, indicating that CL hydrolysis and degradation were increased in the *taz1*Δ strain. *CLD1* deletion in the *taz1*Δ strain produced a significant reduction in the number of cells with fragmented mitochondria, and the *cld1*Δ*taz1*Δ double mutant rescued the mitochondrial defect of the *taz1*Δ strain. One possible explanation for this is that the level of MLCL was reduced in the double mutant compared with the single mutant. *DDL1* deletion in the *taz1*Δ strain caused an increase in the number of cells with fragmented mitochondria. Therefore, the most likely explanation is that CL, PE, and PG remodeling and CL degradation were affected in the double mutant. Interestingly, compared with the *taz1*Δ strain, the *cld1*Δ*ddl1*Δ*taz1*Δ strain showed reduced mitochondrial fragmentation. The CL content was also increased in the triple mutant compared with the *taz1*Δ strain, which can be attributed to the deletion of both CL-preferring lipases. These data suggested that the accumulation of MLCL in the *taz1*Δ strain is deleterious. Like deletion strains in CL metab-

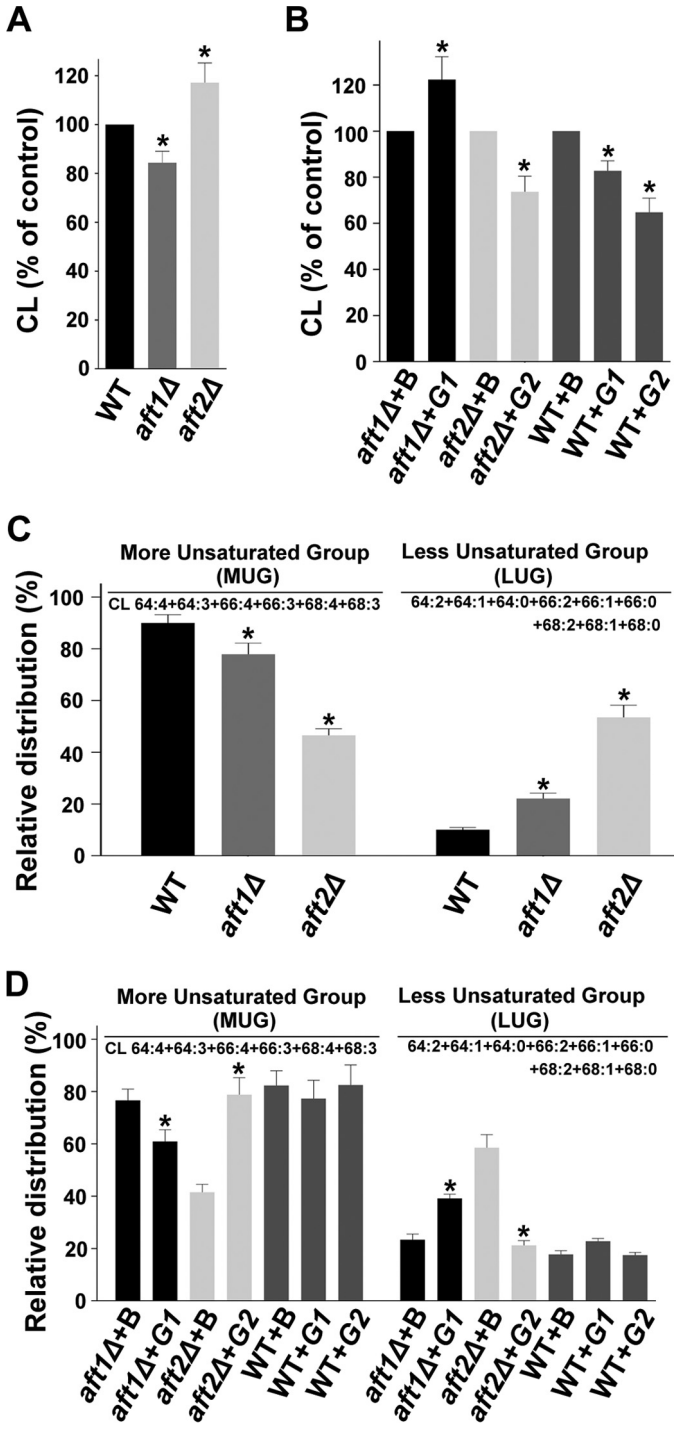

FIGURE 10. **The *AFT1* and *AFT2* genes and cellular CL content.** *A* and *B*, effects of the *AFT1* and *AFT2* genes on the cellular CL content. The lipids that were extracted from the stationary-phase cells (A_{600} = 25) grown in the presence of [^{14}C]acetate were resolved on a TLC plate. *C*, effect of deletion of the *AFT1* and *AFT2* genes on molecular species of CL. The extracted lipids were analyzed by MS/MS^{ALL}. In *C*, the values in the *WT panel* were duplicated from Fig. 4*A* to generate the *graph*. *D*, effects of the *AFT1* and *AFT2* genes on molecular species of CL. The extracted lipids were analyzed by MS/MS^{ALL} (*B*, BG1805 vector; *G1*, BG1805-*AFT1*; and *G2*, BG1805-*AFT2*). The values are presented as the mean ± S.E. (n = 3). Significance was determined at *, $p < 0.05$.

olism, the *DDL1*-defective strains also showed mitochondrial dysfunction. Therefore, the most likely explanation is that CL, PE, and PG remodeling and CL degradation were affected in the *DDL1*-defective strains. Based on our findings, it is clear that both CL remodeling and CL degradation are important for cell survival.

To identify the transcription factor that regulates the *DDL1* gene, we performed an *in silico* analysis and determined that the Aft1/2 transcription factors have the same putative binding site in the upstream region of the *DDL1* promoter. Aft1 negatively regulates *DDL1* expression, whereas Aft2 positively regulates *DDL1* expression. CL profiling in both the deletion and overexpression strains suggested that *AFT1/2* may play a role in CL metabolism. Studies related to mitochondrial function suggested that *AFT1* deletion and *AFT2* overexpression cause similar phenotype, such as fragmented mitochondria. Both deletion/down-regulation and overexpression/up-regulation of *DDL1* are deleterious to the cells. Thus, our entire study can be summarized thus: "the misregulation of *DDL1* by Aft1/2 alters CL metabolism and causes mitochondrial dysfunction in the cells."

Nakajima *et al.* (29) have reported that human DDHD2 hydrolyzes PA and PE, and it prefers PA as a substrate. Inoue *et al.* (4) have shown that both DDHD1 and DDHD2 have PA-PLA1 activity. Mutations in the *DDHD1* and *DDHD2* genes cause HSP (SPG28 and SPG54, respectively), and the deletion of yeast *DDL1* produced similar phenotypes (mitochondrial dysfunction and defects in lipid metabolism). It has been also reported that DDHD1 is partially localized to the mitochondria (6, 30). Therefore, it will be interesting to investigate the role of *DDHD1/2* in CL metabolism. In addition, the *DDL1*-defective strain could be a good model system for understanding hereditary spastic paraplegia.

Experimental Procedures

Materials—The phospholipids used in this study (MLCL; DOPE, 1,2-dioleoyl-*sn*-glycero-3-phosphoethanolamine; SOPE, 1-stearoyl-2-oleoyl-*sn*-glycero-3-phosphoethanolamine; POPE, 1-palmitoyl-2-oleoyl-*sn*-glycero-3-phosphoethanolamine; DOPG, 1,2-dioleoyl-*sn*-glycero-3-phospho-(1′-rac-glycerol); SOPG, 1-stearoyl-2-oleoyl-*sn*-glycero-3-phospho-(1′-rac-glycerol); POPG, 1-palmitoyl-2-oleoyl-*sn*-glycero-3-phospho-(1′-rac-glycerol); TopFluor-CL, 1,1′,2,2′-tetraoleoyl cardiolipin [4-(dipyrrometheneboron difluoride)butanoyl]; NBD-PA, 1-oleoyl-2-{12-[(7-nitro-2–1,3-benzoxadiazol-4 yl)amino]dodecanoyl}-*sn*-glycero-3-phosphate; NBD-PC, 1-oleoyl-2-[12-[(7-nitro-2–1,3-benzoxadiazol-4-yl)amino]dodecanoyl]-sn-glycero-3-phosphocholine; NBD-PG, 1-oleoyl-2-{12-[(7-nitro-2–1,3-benzoxadiazol-4-yl)amino]dodecanoyl}-*sn*-glycero-3-[phosphorac-(1-glycerol)]; and NBD-PS, 1-oleoyl-2-{12-[(7-nitro-2–1,3-benzoxadiazol-4-yl)amino]dodecanoyl}-*sn*-glycero-3-phosphoserine) were purchased from Avanti Polar Lipids Inc. Cardiolipin and NBD-PE (*N*-(NBD-aminohexanoyl)-1,2-dioleoyl-*sn*-glycero-3-phosphoethanolamine)) were obtained from Sigma-Aldrich. [^{14}C]Acetate was obtained from American Radiolabeled Chemicals, Inc. The enzymes used for cloning were procured from New England Biolabs. The protein molecular mass markers were obtained from New England Biolabs and Genetix Biotech Asia Pvt. Ltd., the Ni^{2+}-NTA-agarose columns were purchased from Bio-Rad, and TLC plates were obtained from Merck. The fluorescence-based probes for the yeast mitochondria were purchased from Life Technologies.

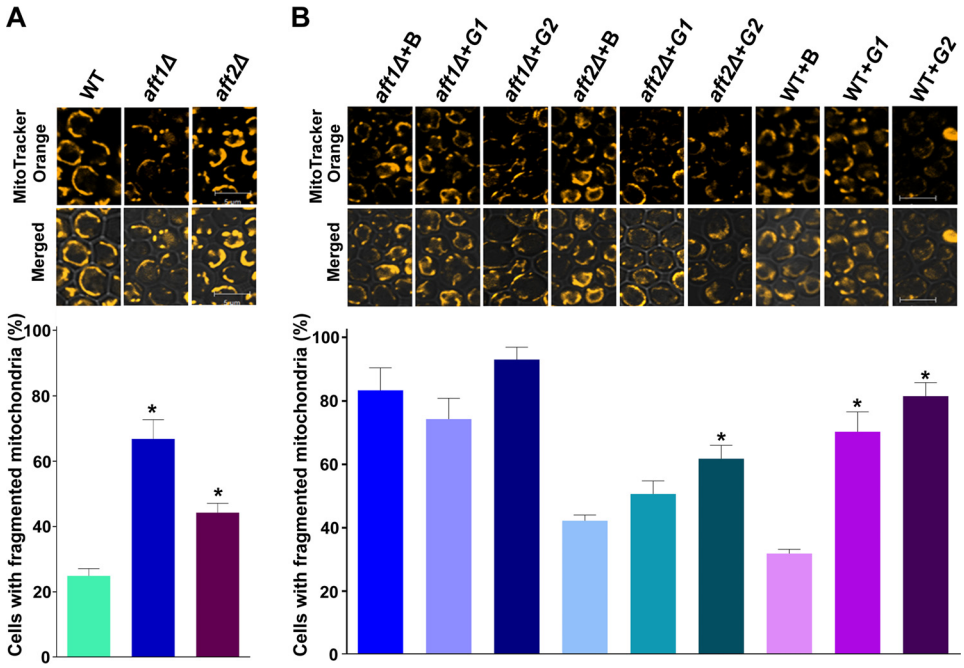

FIGURE 11. **Physiological significance of the *AFT1* and *AFT2* genes.** *A* and *B*, effects of *AFT1* and *AFT2* deletion (*A*) and overexpression (*B*) on mitochondrial morphology. Stationary-phase cells were stained with mitochondrial dye. The images were captured with a confocal microscope *B*, BG1805 vector; *G1*, BG1805-*AFT1*; *G2*, BG1805-*AFT2*. In *A*, the values in the *WT panel* were duplicated from Fig. 8*A*. *Bar*, 5 μm. To quantify mitochondrial fragmentation, at least 200 cells were scored in each background. The values are presented as the mean ± S.E. ($n = 3$). Significance was determined at *, $p < 0.05$.

The materials required for real-time quantitative PCR analysis were purchased from Applied Biosystems. The materials required for yeast extract-peptone-dextrose (YPD) and Luria-Bertani (LB) media were purchased from HiMedia. Yeast nitrogen base was purchased from Difco. The yeast transformation kit was obtained from Clontech. The glass beads, ammonium acetate, yeast synthetic drop-out medium, antibiotic, oligonucleotides, antibodies (H1029 and A3562), and all other reagents were obtained from Sigma-Aldrich unless specified otherwise.

Strains, Plasmids, and Culture Conditions—The strains used in this study are listed in Table 1. The yeast deletion strains were purchased from Euroscarf. The double and triple deletion strains were created using a PCR-based gene deletion protocol (31). The deletion cassette (spanning the whole marker cassette plus the homologous upstream and downstream regions of the targeted gene) was amplified from the YEp351 (*LEU2*) or pUG34 (*HIS3*) vector. The cells were transformed with the PCR product (deletion cassette) to produce homologous recombination, and the positive colonies were confirmed by PCR using the different screening primers listed in Table 2. The plasmids used in this study are listed in Table 3. To create the constructs, the genomic DNA was isolated from yeast cells. Gene-specific primers were used to amplify the *DDL1* (*YOR022C*) gene from the genomic DNA. The gene was cloned into the pYES2/NT B yeast expression vector using the KpnI (forward primer) and XhoI (reverse primer) restriction sites and named as pRP1. The pRP2, pRP3, and pRP4 plasmids were constructed by PCR-mediated site-directed mutagenesis using the pRP1 construct as a template. The truncated *DDL1* (*DDL1* gene devoid of the C-terminal DDHD domain) gene was cloned into the pYES2/NT B vector, and the construct was named pRP5. To analyze the β-galactosidase activity, the pRP6 plasmid was constructed by cloning 1000 base pairs of the upstream promoter sequence plus 9 base pairs downstream of the start site of the *DDL1* gene into the YEp357 vector. KpnI (forward primer) and XbaI (reverse primer) restriction sites were used for cloning. The pRP7 and pRP8 plasmids were constructed by cloning the *AFT1* and *AFT2* genes, respectively, into the pRSET A bacterial expression vector. Gene-specific primers with XhoI (forward primer) and KpnI (reverse primer) restriction sites were used for the PCR amplification of the *AFT1* and *AFT2* genes from the yeast genomic DNA. The BG1805-*AFT1* and BG1805-*AFT2* plasmids were purchased from Thermo Scientific Open Biosystems. All of the constructs were confirmed by DNA sequencing. The primers used in this study are listed in Table 2.

The strains used in this study were maintained as glycerol stocks at −80 °C. The yeast strains are routinely maintained on YPD-agar (1% yeast extract, 2% peptone, 2% glucose, and 2% agar, pH 6.5) plates stored at 4 °C. The working plates were revived periodically. A single colony of the wild-type strain or other strains was precultured from the working YPD plates in 5 ml of YPD liquid medium in a 50-ml culture tube and allowed to grow overnight at 30 °C with constant shaking at 200 rpm in a shaking incubator. An equal amount of cells was taken from the preculture and subcultured in the required volume of SM medium (yeast nitrogen base, 6.7 g; amino acids drop-out, 1.92 g; uracil, 76 mg/liter; and 2% glucose, pH 6.5) at 30 °C. To select the double and triple deletion strains, the appropriate amino acid was removed from the SM medium. Similarly, to maintain the plasmid in the transformants, uracil (U) was omitted from the medium. In this study, cells harboring the pYES2/NT B-*DDL1*, BG1805-*AFT1*, and BG1805-*AFT2* plasmids were precultured in SM − U + 2% glucose medium and subcultured

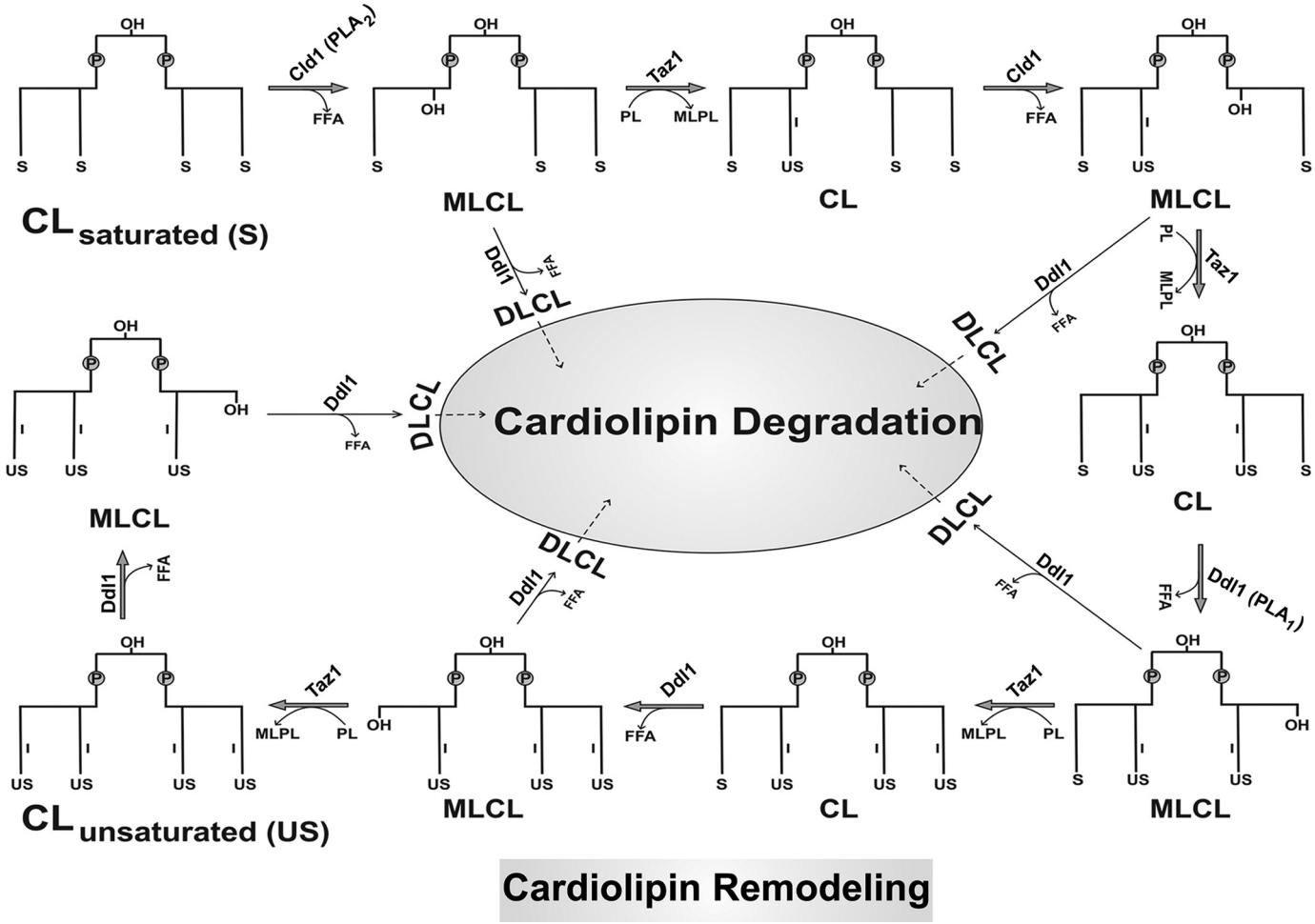

FIGURE 12. **Putative pathway of CL remodeling and degradation in yeast.** We propose that the acyl specificity of CL is achieved by extensive remodeling through PLA_1, PLA_2, and transacylase activities. The dilysocardiolipin (*DLCL*) formed by Ddl1 activity initiates CL degradation. *P*, phosphate group; *S*, saturated fatty acyl chain; *US*, unsaturated fatty acyl chain; *MLPL*, monolysophospholipid.

TABLE 1
Strains used in this study

Strains	Genotypic description	Source
E. coli		
DH5α	F$^-$ ϕ80d*lacZ*ΔM15Δ (*lacZYA-argF*)U169 *deoR recA1 endA1 hsdR17* ($r_k^-m_k^+$) *phoA supE44* λ^-*thi-1 gyrA96 relA1*	Invitrogen
BL21(DE3)pLysS	F$^-$ *ompT hsdS*$_B$ ($r_B^-m_B^-$) *gal dcm* (DE3) pLysS (Cam^R)	Invitrogen
S. cerevisiae		
BY4741	*MATa*; *his3*Δ*1*; *leu2*Δ*0*; *met15*Δ*0*; *ura3*Δ*0*	Euroscarf
ddl1Δ	BY4741; *Mat a*; *his3*Δ*1*; *leu2*Δ*0*; *met15*Δ*0*; *ura3*Δ*0*; *YOR022c::kanMX4*	Euroscarf
cld1Δ	BY4741; *Mat a*; *his3*Δ*1*; *leu2*Δ*0*; *met15*Δ*0*; *ura3*Δ*0*; *YGR110w::kanMX4*	Euroscarf
gep4Δ	BY4741; *Mat a*; *his3*Δ*1*; *leu2*Δ*0*; *met15*Δ*0*; *ura3*Δ*0*; *YHR100c::kanMX4*	Euroscarf
crd1Δ	BY4741; *Mat a*; *his3*Δ*1*; *leu2*Δ*0*; *met15*Δ*0*; *ura3*Δ*0*; *YDL142c::kanMX4*	Euroscarf
taz1Δ	BY4741; *Mat a*; *his3*Δ*1*; *leu2*Δ*0*; *met15*Δ*0*; *ura3*Δ*0*; *YPR140w::kanMX4*	Euroscarf
aft1Δ	BY4741; *Mat a*; *his3*Δ*1*; *leu2*Δ*0*; *met15*Δ*0*; *ura3*Δ*0*; *YGL071w::kanMX4*	Euroscarf
aft2Δ	BY4741; *Mat a*; *his3*Δ*1*; *leu2*Δ*0*; *met15*Δ*0*; *ura3*Δ*0*; *YPL202c::kanMX4*	Euroscarf
ddl1Δ*taz1*Δ	BY4741; *Mat a*; *his3*Δ*1*; *leu2*Δ*0*; *met15*Δ*0*; *ura3*Δ*0*; *YPR140w::kanMX4*; *ddl1*Δ*::LEU2*	This study
cld1Δ*taz1*Δ	BY4741; *Mat a*; *his3*Δ*1*; *leu2*Δ*0*; *met15*Δ*0*; *ura3*Δ*0*; *YPR140w::kanMX4*; *cld1*Δ*::LEU2*	This study
cld1Δ*ddl1*Δ	BY4741; *Mat a*; *his3*Δ*1*; *leu2*Δ*0*; *met15*Δ*0*; *ura3*Δ*0*; *YGR110w::kanMX4*; *ddl1*Δ*::LEU2*	This study
RRY25 (*cld1*Δ*ddl1*Δ*taz1*Δ)	BY4741; *Mat a*; *his3*Δ*1*; *leu2*Δ*0*; *met15*Δ*0*; *ura3*Δ*0*; *YPR140w::kanMX4*; *ddl1*Δ*::LEU2*; *cld1*Δ*::HIS3*	This study

in an induction medium (SM − U + 2% galactose) unless specified otherwise. For the cells that grew slowly, a 3-fold increased amount of the inoculum was subcultured. The bacterial cells were routinely maintained on LB-agar plates (1% tryptone, 0.5% yeast extract, 1% NaCl, and 2% agar) stored at 4 °C. The bacterial cells were cultured in LB medium at 37 °C. Ampicillin (100 μg/ml) was added to the medium to maintain the construct in the cells.

Radiolabeled Precursor Feeding and Lipid Profile Analysis—The yeast cells were grown in SM + U + 2% glucose or SM − U + 2% galactose medium with 0.2 μCi of [^{14}C]acetate/ml. An equal amount of cells (A_{600} = 25) from the stationary phase was taken from each sample for lipid extraction. The lipids were extracted according to the method of Bligh and Dyer (32) with slight modifications. The cells were vigorously vortexed in the presence of a chloroform:methanol:2% orthophos-

TABLE 2
Primers used in this study
qRT, quantitative real-time PCR; p, promoter; d, deletion; F, forward; Sp, screening primer; M, middle; R, reverse; G1, Gly-499; G2, Gly-503.

No.	Gene	Forward primer	Reverse primer
1	*ACT1* (qRT)	ACTTTCAACGTTCCAGCCTTCT	ACACCATCACCGGAATCCAA
2	*AFT1* (qRT)	ATAAGCCCAAAGGACAGGACC	AGGCCCATTGGTTACTGTGG
3	*AFT2* (qRT)	CAACCAAGGCCTGATGGAACT	TGCTTTGTGACAAGGGCCTC
4	*DDL1* (qRT)	GTGTGGTTCGACTCTTCAAATCAA	GGATCATCATTACTGTCGTCGAAT
5	*CLD1* (qRT)	TGCATACGCCCTCGAAAAA	CAATCCGGCGCCATACC
6	*AFT1* (pRSET)	CGGCTCGAGATGGAAGGCTTCAATCCGGCTGACATAG	GAGGTACCCTAATCTTCTGGCTTCACATACT
7	*AFT2* (pRSET)	CGGCTCGAGATGAAAGCAAAGTCGATGA	GAGGTACCTTAATATTTTGATATTAAGGCTGG
8	*DDL1* (pYES2)	AAGGTACCAATGCTACGGTTTACTCATCGAG	TGGCTCGAGTCAACCAGTCTTTCTTTTTACA
9	*tDDL1* (pYES2)		CGGCTCGAGTCATTCATATTTTTTTTGTTT
10	*DDL1* (G1 to Ala)	GTCCATTTAGTGGCTCATTCGTTGGGTAGT	ACTACCCAACGAATGAGCCACTAAATGGAC
11	*DDL1* (Ser to Ala)	CATTTAGTGGGCCATGCTTTGGGTAGTATGA	TCATACTACCCAAAGCATGGCCCACTAAATG
12	*DDL1* (G2 to Ala)	GGGCCATTCGTTGGCTAGTATGATATTATTTG	CAAATAATATCATACTAGCCAACGAATGGCCC
13	*DDL1p* (ChIP)	GATTTGAATGAATATTTGAAGCAACGTGA	GGCCGCTTTTCTTGGTTTCTTGTC
14	*DDL1p* (EMSA)	TTGACGAGCAATAGCGGTATCATCGG	TTCAAGTAATTGTTCACTGTGAGTATATTCAG
15	*DDL1p* (YEp)	AAGGTACC TTGACGAGCAATAGCGGTATC	GCTCTAGACCGTAGCATTTCAAGTAATTGTTC
16	*DDL1d* (*LEU2*)	TTCCCTAATATTGAAGATCACTGAATATACTCACAGT GAACAATTACTTGAAATGAACTGTGGGAATACT	AATAGACAGTAAAGAAAAAAGTTAAAAAAAACTTGTGCCTTGCGTTTACT GATCACAAATTAGGGATTCG
17	*LEU2* cassette	ATATTCTAGAAACTGTGGGAATACTCAGGTATCG	ATATGTCGACCAAATTAGGGATTCGTAGTTTCATGATTTTCTG
18	*DDL1* 5′ FSp		
19	*LEU2* M RSp		CCAAATGCGGTGTTCTTGTCTGGCAAAGAG
20	*LEU2* M FSp	CTCTTTGCCAGACAAGAACACCGCATTT	
21	*DDL1* 3′ RSp		CAACATCTAATAAGCAAAGGGCATTGCTC
22	*DDL1* M Sp	GGGAAAGTCCATTTAGTGGGC	ACGCTGCAATATCCGGTTCT
23	*CLD1d* (*LEU2*)	GTACACTAATACTTATACTGATTAATAAGGGTTAGCCTTT TAATGAACTGTGGGAATACTCAGG	GGCGAAAATGTATGTAAAAATTTCGTTATATAATGTAGATGCACAAGAT TTCTTCATTACAAATTAGGGATTCGTAG
24	*CLD1* 5′ FSp	TGTCAGTGTTTAGCCTCTTTCACCTTTGC	
25	*CLD1* 3′ RSp		AGCCCAACTACTCCATAAAGACAGTGGTTC
26	*CLD1* M Sp	CAAGAACGAGGATGCATTCCA	GACATACCACCAAGGAGGCG
27	*CLD1d* (*HIS3*)	GTACACTAATACTTATACTGATTAATAAGGGTTAGCCTTT TAATGAATTCTCGTTTTAAGAGCTTGG	TAAAAATTTCGTTATATAATGTAGATGCACAAGATTTCTTCATTATGA CACGTATAGAATGATGC
28	*HIS3* cassette	AATGAATTCAATTCTCGTTTTAAGAGCTTG	GCTAAAGCTTTGACACGTATAGAATGATGC
29	*HIS3* M RSp		CGCAGTCTTCAGTGGTGTGATGGTCGT
30	*HIS3* M FSp	ACGACCATCACACCACTGAAGACTGCG	

TABLE 3
Plasmids used in this study

Plasmids	Construct description	Source
pYES2/NT B	Yeast expression vector with N-terminal His_6 tag fusion	Invitrogen
pRSET A	*E. coli* expression vector with N-terminal His_6 tag fusion	Invitrogen
YEp 351	Yeast expression vector with leucine selection	ATCC
YEp 357	Yeast episomal plasmids with *lacZ* reporter gene	ATCC
pUG34	Yeast expression vector with histidine selection	Cathal Wilson
pRP1	*DDL1* gene is cloned into pYES2/NT B: pYES2/NT B-*DDL1* (wild-type)	This study
pRP2	Derived from pRP1 in which ^{1495}GGC^{1497} is mutated to ^{1495}GCT^{1497}: pYES2/NT B-*DDL1* (G1 to A)	This study
pRP3	Derived from pRP1 in which ^{1501}TCG^{1503}is mutated to ^{1501}GCT^{1503}: pYES2/NT B-*DDL1*(S to A)	This study
pRP4	Derived from pRP1 in which ^{1507}GGT^{1509} is mutated to ^{1507}GCT^{1509}: pYES2/NT B-*DDL1* (G2 to A)	This study
pRP5	Truncated *DDL1* gene is cloned into pYES2/NT B: pYES2/NT B-*DDL1*-DDHD (*DDL1* gene devoid of C-terminal DDHD domain)	This study
pRP6	P_{DDL1}-*lacZ* reporter gene containing the *DDL1* promoter into YEp357	This study
pRP7	*AFT1* gene is cloned into pRSETA (pRSET A-*AFT1*)	This study
pRP8	*AFT2* gene is cloned into pRSETA (pRSET A-*AFT2*)	This study
BG1805	Yeast expression vector with uracil selection	Open Biosystems
BG1805-*AFT1*	*AFT1* gene is cloned into BG1805	Open Biosystems
BG1805-*AFT2*	*AFT2* gene is cloned into BG1805	Open Biosystems

phoric acid (1:2:1, v/v) solution and acid-washed glass beads. The total lipids were extracted using the chloroform:methanol: 2% orthophosphoric acid (1:1:1, v/v) solution and re-extracted again in the same mixture. The extracted lipids were dried in a SpeedVac concentrator. To separate PA, PC, PE, PI, PS, CL, and PG, the extracted lipids were analyzed on a TLC plate using solvent system 1 (chloroform:methanol:acetic acid:water, 85:15:10:3.5, v/v). The plate was placed in a phosphorimaging screen cassette and scanned in a Typhoon FLA 9500 laser scanner (GE Healthcare). To separate CL and PG from the other phospholipids, the extracted lipids were analyzed on a TLC plate using solvent system 2 (chloroform:methanol:glacial acetic acid, 65:25:8, v/v), followed by phosphorimaging. To separate CL and PG, solvent system 3, which is a two-dimensional system (a basic solvent system followed by an acidic system), was also used. The first dimension was chloroform:methanol: 25% ammonia (65:35:4, v/v), and the second dimension was chloroform:methanol:acetic acid:water (85:25:5:4, v/v). Each phospholipid species was scraped off of the plate, and the label was counted with a liquid scintillation counter (PerkinElmer Micro Beta^2 2450 microplate counter) using a toluene-based scintillation fluid. As reported earlier (33), the amount of each phospholipid species was determined relative to the total phospholipid content, and each phospholipid species in a strain was compared with WT/control values that were set at 100%. To separate MLCL from the other phospholipids, the cells were grown to the stationary phase, and the lipids were extracted from 50 mg of lyophilized cells. The extracted lipids were

resolved using solvent system 4 (chloroform:methanol:acetic acid:water, 85:25:5:4, v/v), and the plate was then charred with 10% cupric sulfate in 8% aqueous phosphoric acid solution for 10 min at 180 °C. CL and MLCL were quantified using GeneTools software (SynGene, a division of Synoptics Ltd.). The amounts of CL and MLCL were determined relative to the total CL (CL + MLCL) content and represented as a percentage for comparison.

Expression and Purification of the Recombinant Proteins—The proteins were expressed according to the protocol given for the respective cloning vector, with slight modifications. Yeast cells harboring the pYES2/NT B-*DDL1* construct were grown overnight in 10 ml of SM − U + 2% glucose medium at 30 °C with shaking. On the next day, the cells were pelleted, washed with autoclaved water, and grown in 50 ml of SM − U + 2% raffinose medium overnight at a starting A_{600} of 0.4. Again, the cells were pelleted, washed with the autoclaved water, and transferred to 400 ml of SM − U + 2% raffinose medium for growth. At A_{600} = 0.8–1.2, 200 ml of 3× YPG (3% yeast extract, 6% peptone, and 6% galactose, pH 6.5) induction medium was added to the culture and grown for 6 h. The rich induction medium (3× YPG) was used to produce a higher yield of the protein (34). The cells were pelleted by centrifugation at 4 °C and suspended in 20 ml of yeast lysis buffer containing 50 mM Tris-HCl, pH 8.0, 300 mM NaCl, 5 mM $MgCl_2$, 1 mM PMSF, and 10% glycerol (v/v). The cells were lysed at 4 °C using glass beads. The His-tagged protein was affinity-purified according to the manufacturer's recommendation (Bio-Rad). The lysed sample was subjected to high speed centrifugation (10000 × *g*) for 30 min at 4 °C. The supernatant containing the recombinant protein was allowed to bind to the Ni^{2+}-NTA matrix. The column was washed with wash buffer 1 containing 50 mM Tris-HCl, pH 8.0, 300 mM NaCl, and 20 mM imidazole followed by a second wash with wash buffer 2 containing 50 mM Tris-HCl, pH 8.0, 300 mM NaCl, and 40 mM imidazole. The bound protein was eluted with buffer containing 50 mM Tris-HCl, pH 8.0, 300 mM NaCl, and 150 mM imidazole. The fractions (1 ml each) were collected and analyzed by 12% SDS-PAGE followed by Coomassie Brilliant Blue staining, and the proteins were confirmed by immunoblot analysis using an anti-His_6 monoclonal antibody. The purified protein was subjected to dialysis, and the protein concentration was measured using Lowry's method.

Escherichia coli BL21(DE3)pLysS cells harboring the pRSET A-*AFT1* and pRSET A-*AFT2* plasmids were precultured in 5 ml of LB medium with 100 μg/ml ampicillin and 34 μg/ml chloramphenicol overnight at 37 °C. The cells from the preculture were then inoculated in 1000 ml of LB medium containing 100 μg/ml ampicillin, 34 μg/ml chloramphenicol, 1 mM betaine, and 0.5 M sorbitol (35). The bacterial cells were grown at 37 °C to an A_{600} of 0.6–0.9 and induced with 0.5 mM isopropyl β-D-thiogalactopyranoside for 12 h at 16 °C. To enable proper folding of the recombinant protein, 200 μM $ZnCl_2$ was also added to the induction medium (36). The cells were pelleted, and the pellet was suspended in bacterial lysis buffer containing 50 mM Tris-HCl, pH 8.0, 300 mM NaCl, 10 mM imidazole, 1 mM PMSF, and 10% glycerol (v/v). The cells were lysed by sonication, and the lysed sample was subjected to high speed centrifugation (10000 × *g*) for 20 min at 4 °C. The supernatant containing the recombinant protein was allowed to bind to the Ni^{2+}-NTA matrix, and the protein was purified similar to the recombinant yeast protein. The protein samples were analyzed by 12% SDS-PAGE followed by Coomassie Brilliant Blue staining. The purified protein was subjected to dialysis and then used for further studies.

Site-directed Mutagenesis—Site-directed mutagenesis was conducted to evaluate the role of the G*X*S*X*G motif in the lipase activity. The predicted amino acid residues Gly-499, Ser-501, and Gly-503 were replaced with alanine (Ala). The mutations in the lipase motif were produced by PCR-based amplification of the entire pRP1 construct. The primers used in this experiment are listed in Table 2. The mutated codon is underlined in the primer sequence. A QuikChange Lightning site-directed mutagenesis kit (Agilent Technologies) was used to construct the mutants, which were confirmed by the DNA sequencing.

Phospholipase Assay—Phospholipase activity was measured under different assay conditions using 5 μM fluorescently tagged CL, PE, and PG substrates. A protein-dependent assay was conducted with increasing amounts of the purified Ddl1 protein for 10 min at 30 °C, and a time-dependent assay was performed in the presence of 1 μg of the purified Ddl1 protein. For the pH-dependent assay, the activity was conducted at different pH values in the Bistris propane buffer system in the presence of 1 μg of the purified protein for 10 min at 30 °C. For the temperature-dependent assay, the activity was analyzed for 10 min at different temperatures in the presence of 1 μg of the purified Ddl1 protein. The assay mixture consisted of 50 mM Tris, pH 8.0, 3 mM $MgCl_2$, 1 mM EDTA, 5 mM $CaCl_2$, 250 μM CHAPS, 40% glycerol, 5 μM fluorescently labeled substrate, and 1 μg of the purified Ddl1 protein in a total volume of 100 μl. Under each assay condition, the reaction was stopped, and lipids were resolved on a TLC plate using chloroform:methanol:25% ammonia (65:25:5, v/v) as solvent system 5, which was used to separate the phospholipids and free fatty acids (FFA) on a single TLC plate. The TLC plates were visualized in a Typhoon FLA 9500 laser scanner, and the lipid molecules were quantified using GeneTools software.

The phospholipase activity of Ddl1 was measured by estimating the FFA release using a fluorescent FFA estimation kit (Cayman Chemical) as reported by Vijayakumar *et al.* (37). Nonfluorescent (native) PE and PG with different fatty acid compositions were also used for the assays. The released FFA was scraped from the TLC plates, and the samples were prepared and subjected to gas chromatographic (GC) analysis. The protocols used to prepare the fatty acid methyl esters and separate them on the GC system were performed as reported by Yadav *et al.* (38). Briefly, the scraped FFA band containing silica was derivatized with 1 ml of boron trifluoride-methanol for the GC analysis. The fatty acid methyl esters were separated with a DB-Wax-23 column as follows: 50 °C for 2 min, and then the temperature was raised to 180 °C at a rate of 5 °C/min, and thereafter it was raised to 240 °C at a rate of 5 °C/min. The samples were maintained at 240 °C for 5 min, and then the temperature was raised to 300 °C at a rate of 30 °C/min and maintained at 300 °C for 5 min. The total run time was 34 min.

TABLE 4
Parameters for identification of molecular species of phospholipids by PeakView software

Parameters	Fragment ion	Polarity
Precursor ion (*m/z*)		
PC head	184.1	Positive
PE head	196.1	Positive
PA head	153.1	Negative
PG head	153.1	Negative
PS head	153.1	Negative
CL building block head	153.1	Negative
PI head	241.1	Negative
PI head	259.2	Negative
FA 12:0	199.2	Negative
FA 14:0	227.2	Negative
FA 16:0	255.2	Negative
FA 16:1	253.2	Negative
FA 18:0	283.3	Negative
FA 18:1	281.3	Negative
Neutral loss (*m/z*)		
PE	141.1	Positive
PI	227.2	Negative
PG	189.1	Negative
PS	185.1	Negative
Serine-H_2O	87.1	Negative

The recombinant mutant and truncated Ddl1 proteins were also used to measure the phospholipase activity.

Lipidomic Analysis by Mass Spectrometry—The yeast cells were grown in 100 ml of their respective SM medium in a 500-ml conical flask. For the lipidome analysis, the cells were harvested from the stationary phase and lyophilized. To identify the molecular species of PA, PC, PE, PG, PI, PS, and CL, an equal amount of lyophilized cells (10 mg) was taken from each sample for lipid extraction. The dried lipids were dissolved in 250 μl of chloroform:methanol (1:2) plus 7.5 mM ammonium acetate and diluted 10-fold. The samples were analyzed using MS/MS^{ALL} on an AB Sciex TripleTOF^{TM} 5600 system. The samples were directly infused at a flow rate of 7 μl/min. The molecular species of PC and PE were identified in the positive mode, whereas the species of PA, PG, PI, PS, and CL were analyzed in the negative mode. The major CL molecular species clusters (CL C64 to C68) were grouped into two groups, the MUGs and the LUGs.

In each case, the molecular species were annotated by their sum:composition (total fatty acyl carbons:total fatty acyl double bonds). The molecular species identifications and relative quantifications were performed using the LipidView and PeakView software packages (AB Sciex). The molecular species identified by the LipidView software were verified with PeakView software using a manual fragmentation analysis. The precursor ions and neutral loss scan parameters listed in Table 4 were used in the PeakView software analyses.

In the MS/MS^{ALL} technique, a TOF-MS experiment (to scan from *m/z* 200–1200) was followed by product ion analyses (1,000 individual MS/MS experiments), as reported by Simons *et al.* (39) and Huang *et al.* (40). The parameters for the TOF-MS experiment include ion source gas 1 (GS1) at 15 psi, ion source gas 2 (GS2) at 20 psi, curtain gas (CUR) at 25 psi, an ESI source temperature of 200 °C, ion spray voltage at +5100 (positive) or −4500 (negative) V, and an accumulation time of 3000 ms. A declustering potential of ±80 V and a collision energy of ±10 eV were used for the positive and negative ion mode experiments, respectively. The parameters for the product ion experiments include similar source/gas values as for the TOF-MS experiment and an accumulation time of 300 ms. A declustering potential of ±80 V and a collision energy of ±50 eV were used for the positive and negative ion mode experiments, respectively. The other parameters include a collision energy spread of 30, an ion release delay of 30, and an ion release width of 15. The TripleTOF^{TM} 5600 system was calibrated using mode-specific calibration solutions (AB Sciex). A wash step was included between each sample to remove any carryover.

RNA Preparation and Real-time Quantitative PCR Analysis—An equal amount of yeast cells (A_{600} = 25) from the stationary phase was collected and stored in RNA*later* at −20 °C. An RNA isolation kit (NucleoSpin® RNA II kit, Macherey-Nagel) was used to isolate the total RNA, and the quality and the quantity of the RNA were checked by a NanoDrop spectrophotometer. A high capacity cDNA reverse transcription kit (Applied Biosystems) was used to prepare the complementary DNAs (cDNAs). The cDNAs were synthesized from 1 μg of RNA according to the manufacturer's protocol. The primers used in this experiment (listed in Table 2) were designed with the help of the Primer Express® software 3.0 (Applied Biosystems). The cDNAs were diluted at 1:25, and 1 μl of the diluted cDNA was used for the real-time quantitative PCR analysis. The real-time PCR assays were conducted in triplicate on an ABI PRISM 7700 sequence detection system (Applied Biosystems) using the cDNAs, gene-specific primers, and 1× Power SYBR® Green PCR master mix (Applied Biosystems). Gene expression was normalized using actin (*ACT1*) as an endogenous control. The real-time quantitative PCR data are represented as the fold change of the control value, which was set to 1.

β-Galactosidase Assay—The YEp357 vector and pRP6 (YEp357-*DDL1*) construct were transformed into the WT, *aft1*Δ, and *aft2*Δ strains. To assess the β-galactosidase activity of *DDL1-lacZ* on the WT, *aft1*Δ and *aft2*Δ backgrounds, the transformants were grown in SM medium designed to maintain selection of the plasmid. Cells from the different transformants were collected and washed with water. The cell-free extracts were prepared, and the β-galactosidase activity was measured using a standard protocol (41). The β-galactosidase activity under the control of the *DDL1* promoter in the *aft1*Δ and *aft2*Δ strains was represented as a percentage of the activity in the WT strain, which was set at 100%.

ChIP Assay—ChIP assays were performed using a Dynabeads co-immunoprecipitation kit (Invitrogen) with some adaptations taken from van Attikum *et al.* (42). Briefly, the transformants (BG1805-*AFT1/2*) overexpressing Aft1/2 proteins were collected from the late log phase in 50-ml culture tubes, and cells were fixed with formaldehyde at a 1% final concentration for 15 min. An excess amount of formaldehyde was quenched with 2.5 M glycine. Cells were washed with 1× PBS, pH 7.4, and pellets were stored at −80 °C until use. ChIP-grade monoclonal anti-HA (H3663, lot 025M4772V) and anti-RFP (SAB2702214, lot 41232) antibodies from Sigma-Aldrich were used in the assays. The anti-HA antibody coating on the Dynabeads was done according to the manufacturer's recommendation. Similarly, for the control assay, Dynabeads with the anti-RFP anti-

body were also processed and antibody-coated beads were kept at 4 °C until use. The following steps were performed at 4 °C. Cell extracts were prepared in the extraction buffer by vortexing in the presence of glass beads, protease inhibitor mixture (P8215), and PMSF from Sigma-Aldrich, and cell extracts were collected. A Sonics Vibra-Cell sonicator was used to obtain chromatin fragments of 300 to 700 bp. For the sonication, we used 15 cycles of 3 s "on" and 30 s "off" at 30% amplitude followed by 5 cycles of 10 s on and 60 s off at 20% amplitude. To prevent reverse cross-linking, the cell extracts were kept in ice during the sonication. For the recovery of the sonicated chromatin, a hole was made with a needle in the tube containing the sonicated samples. The sonicated samples were recovered by centrifugation at 2000 rpm for 5 min at 4 °C. The samples were transferred to the new tubes and centrifuged at 13,000 rpm for 15 min at 4 °C. In each case, the supernatant was transferred to the new tube and centrifuged again at 13,000 rpm for 15 min at 4 °C. In each case, the supernatant was collected, and about one-tenth of the total chromatin was kept at −20 °C for input; the rest of the chromatin was divided into two parts, one as immunoprecipitated (IP) and other as control immunoprecipitated (CIP). The IP and CIP samples were incubated for 45 min at 4 °C with the Dynabeads coated with anti-HA and anti-RFP antibodies, respectively. After incubation, the Dynabeads were washed with extraction and wash buffers. DNA recovery from input, IP, and CIP was done using a PCR cleanup kit (Sigma-Aldrich). PCR-based data analysis was performed, and the PCR product band intensities were quantified by densitometric analysis using the GeneTools software. The obtained results were represented as reported earlier (43). Final concentrations of 1% (input) and 4% (IP and CIP) were used as a template for the PCR reaction. Primers used in the ChIP assays are listed in Table 2.

Electrophoretic Mobility Shift Assay—To identify the regulatory relationship between Aft1/2 transcription factors and the *DDL1* gene, EMSAs were performed for the *DDL1* promoter using an EMSA kit (Molecular Probes) with slight modifications. The EMSA binding buffer consisted of 4 mM Tris, pH 7.5, 12 mM HEPES, pH 7.5, 75 mM KCl, 5 mM $MgCl_2$, 1 mM DTT, 100 μM $ZnCl_2$, 0.1 mg/ml poly(dI-dC), 0.1 mg/ml BSA, and 7.5% glycerol. The *DDL1* promoter (1 kb) was amplified using the primers listed in Table 2. Bacterially expressed and purified Aft1/2 proteins were used for this study. A protein-dependent EMSA was performed with an increasing amount of the purified Aft1/2 proteins (200 ng to 1 μg) in the presence of 200 ng of the *DDL1* promoter DNA at 30 °C for 1 h. In each assay, one reaction was performed in the presence of an anti-His_6 monoclonal Ab. The EMSA was also performed with the purified Aft1/2 proteins (1 μg) in the presence of 200 ng of the *DDL1* promoter DNA (1 kb) and Ab or Fe^{2+}. Fe^{2+} was used to inhibit the Aft1/2 binding (36). After the DNA-protein complex formed at 30 °C, the samples were resolved on a 6% nondenaturing polyacrylamide gel in 0.5× TBE buffer (Tris borate-EDTA) at 4 °C in a cold room. The gel was stained with SYBR® Green EMSA nucleic acid stain, and the images were documented with a UV transilluminator at 300 nm.

Confocal Microscopic Study—The stationary-phase cells grown in SM medium were collected to assess the mitochondrial morphology. The cells from different genetic backgrounds were collected, washed, and stained with the mitochondrial dye MitoTracker Orange CMTMRos at 100 nM in 10 mM HEPES buffer containing 5% glucose, pH 7.4. The images were captured with a confocal microscope. In each case, the microscope slides were coated with a very thin film of agarose. A Zeiss LSM 700 confocal laser-scanning microscope was used to image the cells.

Measurement of Mitochondrial Membrane Potential—To measure the mitochondrial membrane potential, the potentiometric dye JC-1 (Sigma-Aldrich) was used as described previously (44). The JC-1 dye is accumulated as red fluorescent J-aggregates in the functional mitochondria in a potential-dependent manner. To assess the mitochondrial membrane potential, cells of different genetic backgrounds were collected from the stationary phase and washed with SM medium. Equal amounts of the washed cells were resuspended in SM medium with JC-1 stain (5 μg/ml) and incubated for 30 min at 30 °C in the dark. After incubation, the cells were pelleted, washed with SM medium, and resuspended in this medium. Finally, an equal volume of cells suspended in the medium was transferred to a 96-well plate to measure their fluorescence. A Thermo Scientific Varioskan Flash multimode fluorescence plate reader was used to measure red (550/600) and green (485/535) fluorescence. The ratio of F_{red} to F_{green} was used to determine the relative mitochondrial membrane potential. Cells with healthy and functional mitochondria showed a higher red to green fluorescence ratio, whereas a decrease in the red/green fluorescence ratio indicated the presence of dysfunctional mitochondria. The mitochondrial membrane potential was represented as a percentage of the control value, which was set to 100%.

Measurement of Oxygen Consumption—Cells of different genetic backgrounds were collected from the stationary phase and washed with the SM medium. A closed chamber equipped with a Clark-type oxygen electrode (Strathkelvin Instruments, model 782) was used to measure the oxygen consumption rate of the whole yeast cells at 30 °C for 5 min with constant agitation. An equal amount of cells was used to measure the rate of oxygen consumption, represented as a percentage of the control value, which was set at 100%.

Statistical Analysis—The experimental data are shown as the mean ± S.E., and data were analyzed using Student's *t* test. Each experiment was repeated at least three times, and at least 200 cells were scored in each strain per experiment to quantify the microscopic data. Significance was determined at *, $p < 0.05$; and **, $p < 0.01$.

Author Contributions—R. R. conceived and initiated the project. R. R. and P. K. Y. designed the experiments. P. K. Y. executed the experiments and analyzed the data. P. K. Y. and R. R. discussed the data and wrote the paper.

Acknowledgments—We are grateful to Prof. Vasanthi Nachiappan, Department of Biochemistry, Bharathidasan University, India for providing pUG34 vector. We also are grateful to the Department of Biochemistry, Indian Institute of Science, Bangalore, for help with the radioactive study.

References

1. Lev, S. (2004) The role of the Nir/rdgB protein family in membrane trafficking and cytoskeleton remodeling. *Exp. Cell Res.* **297,** 1–10
2. Tani, K., Kogure, T., and Inoue, H. (2012) The intracellular phospholipase A1 protein family. *Biomol. Concepts* **3,** 471–478
3. Higgs, H. N., and Glomset, J. A. (1994) Identification of a phosphatidic acid-preferring phospholipase A1 from bovine brain and testis. *Proc. Natl. Acad. Sci. U.S.A.* **91,** 9574–9578
4. Inoue, H., Baba, T., Sato, S., Ohtsuki, R., Takemori, A., Watanabe, T., Tagaya, M., and Tani, K. (2012) Roles of SAM and DDHD domains in mammalian intracellular phospholipase A1 KIAA0725p. *Biochim. Biophys. Acta* **1823,** 930–939
5. Inloes, J. M., Hsu, K. L., Dix M. M., Viader, A., Masuda, K., Takei, T., Wood, M. R., and Cravatt, B. F. (2014) The hereditary spastic paraplegia-related enzyme DDHD2 is a principal brain triglyceride lipase. *Proc. Natl. Acad. Sci. U.S.A.* **111,** 14924–14929
6. Tesson, C., Nawara, M., Salih, M. A., Rossignol, R., Zaki, M. S., Al Balwi, M., Schule, R., Mignot, C., Obre, E., Bouhouche, A., Santorelli, F. M., Durand, C. M., Oteyza, A. C., El-Hachimi, K. H., Al Drees, A., *et al*. (2012) Alteration of fatty-acid-metabolizing enzymes affects mitochondrial form and function in hereditary spastic paraplegia. *Am. J. Hum. Genet.* **91,** 1051–1064
7. Gonzalez, M., Nampoothiri, S., Kornblum, C., Oteyza, A. C., Walter, J., Konidari, I., Hulme, W., Speziani, F., Schöls, L., Züchner, S., and Schüle, R. (2013) Mutations in phospholipase DDHD2 cause autosomal recessive hereditary spastic paraplegia (SPG54). *Eur. J. Hum. Genet.* **21,** 1214–1218
8. Blackstone, C. (2012) Cellular pathways of hereditary spastic paraplegia. *Annu. Rev. Neurosci.* **35,** 25–47
9. Dimmer, K. S., and Scorrano, L. (2006) (De)constructing mitochondria: what for? *Physiology* **21,** 233–241
10. Schuiki, I., and Daum, G. (2009) Phosphatidylserine decarboxylases, key enzymes of lipid metabolism. *IUBMB Life* **61,** 151–162
11. Claypool, S. M., and Koehler, C. M. (2012) The complexity of cardiolipin in health and disease. *Trends Biochem. Sci.* **37,** 32–41
12. Joshi, A. S., Thompson, M. N., Fei, N., Hüttemann, M., and Greenberg, M. L. (2012) Cardiolipin and mitochondrial phosphatidylethanolamine have overlapping functions in mitochondrial fusion in *Saccharomyces cerevisiae*. *J. Biol. Chem.* **287,** 17589–17597
13. Jiang, F., Ryan, M. T., Schlame, M., Zhao, M., Gu, Z., Klingenberg, M., Pfanner, N., and Greenberg, M. L. (2000) Absence of cardiolipin in the crd1 null mutant results in decreased mitochondrial membrane potential and reduced mitochondrial function. *J. Biol. Chem.* **275,** 22387–22394
14. Gohil, V. M., Thompson, M. N., and Greenberg, M. L. (2005) Synthetic lethal interaction of the mitochondrial phosphatidylethanolamine and cardiolipin biosynthetic pathways in *Saccharomyces cerevisiae*. *J. Biol. Chem.* **280,** 35410–35416
15. Vreken, P., Valianpour, F., Nijtmans, L. G., Grivell, L. A., Plecko, B., Wanders, R. J., and Barth, P. G. (2000) Defective remodeling of cardiolipin and phosphatidylglycerol in Barth syndrome. *Biochem. Biophys. Res. Commun.* **279,** 378–382
16. Schlame, M., Kelley, R. I., Feigenbaum, A., Towbin, J. A., Heerdt, P. M., Schieble, T., Wanders, R. J., DiMauro, S., and Blanck, T. J. (2003) Phospholipid abnormalities in children with Barth syndrome. *J. Am. Coll. Cardiol.* **42,** 1994–1999
17. Beranek, A., Rechberger, G., Knauer, H., Wolinski, H., Kohlwein, S. D., and Leber, R. (2009) Identification of a cardiolipin-specific phospholipase encoded by the gene *CLD1* (YGR110W) in yeast. *J. Biol. Chem.* **284,** 11572–11578
18. Ye, C., Lou, W., Li, Y., Chatzispyrou, I. A., Hüttemann, M., Lee, I., Houtkooper, R. H., Vaz, F. M., Chen, S., and Greenberg, M. L. (2014) Deletion of the cardiolipin-specific phospholipase Cld1 rescues growth and life span defects in the tafazzin mutant: implications for Barth syndrome. *J. Biol. Chem.* **289,** 3114–3125
19. Nie, J., Hao, X., Chen, D., Han, X., Chang, Z., and Shi, Y. (2010) A novel function of the human CLS1 in phosphatidylglycerol synthesis and remodeling. *Biochim. Biophys. Acta* **1801,** 438–445
20. Reinders, J., Zahedi, R. P., Pfanner, N., Meisinger, C., and Sickmann, A. (2006) Toward the complete yeast mitochondrial proteome: multidimensional separation techniques for mitochondrial proteomics. *J. Proteome Res.* **5,** 1543–1554
21. Gu, Z., Valianpour, F., Chen, S., Vaz, F. M., Hakkaart, G. A., Wanders, R. J., and Greenberg, M. L. (2004) Aberrant cardiolipin metabolism in the yeast *taz1* mutant: a model for Barth syndrome. *Mol. Microbiol.* **51,** 149–158
22. Schneiter, R., Brügger, B., Sandhoff, R., Zellnig, G., Leber, A., Lampl, M., Athenstaedt, K., Hrastnik, C., Eder, S., Daum, G., Paltauf, F., Wieland, F. T., and Kohlwein, S. D. (1999) Electrospray ionization tandem mass spectrometry (ESI-MS/MS) analysis of the lipid molecular species composition of yeast subcellular membranes reveals acyl chain-based sorting/remodeling of distinct molecular species en route to the plasma membrane. *J. Cell Biol.* **146,** 741–754
23. Berthelet, S., Usher, J., Shulist, K., Hamza, A., Maltez, N., Johnston, A., Fong, Y., Harris, L. J., and Baetz, K. (2010) Functional genomics analysis of the *Saccharomyces cerevisiae* iron-responsive transcription factor Aft1 reveals iron-independent functions. *Genetics* **185,** 1111–1128
24. Rutherford, J. C., Jaron, S., and Winge, D. R. (2003) Aft1p and Aft2p mediate iron-responsive gene expression in yeast through related promoter elements. *J. Biol. Chem.* **278,** 27636–27643
25. Pokorná, L., Čermáková, P., Horváth, A., Baile, M. G., Claypool, S. M., Griač, P., Malínský, J., and Balážová, M. (2016) Specific degradation of phosphatidylglycerol is necessary for proper mitochondrial morphology and function. *Biochim. Biophys. Acta* **1857,** 34–45
26. Chicco, A. J., and Sparagna, G. C. (2007) Role of cardiolipin alterations in mitochondrial dysfunction and disease. *Am. J. Physiol. Cell Physiol.* **292,** C33–C44
27. Riekhof, W. R., Wu, J., Jones, J. L., and Voelker, D. R. (2007) Identification and characterization of the major lysophosphatidylethanolamine acyltransferase in *Saccharomyces cerevisiae*. *J. Biol. Chem.* **282,** 28344–28352
28. Tamaki, H., Shimada, A., Ito, Y., Ohya, M., Takase, J., Miyashita, M., Miyagawa, H., Nozaki, H., Nakayama, R., and Kumagai, H. (2007) LPT1 encodes a membrane-bound *O*-acyltransferase involved in the acylation of lysophospholipids in the yeast *Saccharomyces cerevisiae*. *J. Biol. Chem.* **282,** 34288–34298
29. Nakajima, K., Sonoda, H., Mizoguchi, T., Aoki, J., Arai, H., Nagahama, M., Tagaya, M., and Tani, K. (2002) A novel phospholipase A1 with sequence homology to a mammalian Sec23p-interacting protein, p125. *J. Biol. Chem.* **277,** 11329–11335
30. Yamashita, A., Kumazawa, T., Koga, H., Suzuki, N., Oka, S., and Sugiura, T. (2010) Generation of lysophosphatidylinositol by DDHD domain containing 1 (DDHD1): possible involvement of phospholipase D/phosphatidic acid in the activation of DDHD1. *Biochim. Biophys. Acta* **1801,** 711–720
31. Rothstein, R. (1991) Targeting, disruption, replacement, and allele rescue: integrative DNA transformation in yeast. *Methods Enzymol.* **194,** 281–301
32. Bligh, E. G., and Dyer, W. J. (1959) A rapid method of total lipid extraction and purification. *Can. J. Biochem. Physiol.* **37,** 911–917
33. Tamura, Y., Onguka, O., Hobbs, A. E., Jensen, R. E., Iijima, M., Claypool, S. M., and Sesaki, H. (2012) Role for two conserved intermembrane space proteins, Ups1p and Ups2p, in intra-mitochondrial phospholipid trafficking. *J. Biol. Chem.* **287,** 15205–15218
34. Gelperin, D. M., White, M. A., Wilkinson, M. L., Kon, Y., Kung, L. A., Wise, K. J., Lopez-Hoyo, N., Jiang, L., Piccirillo, S., Yu, H., Gerstein, M., Dumont, M. E., Phizicky, E. M., Snyder, M., and Grayhack, E. J. (2005) Biochemical and genetic analysis of the yeast proteome with a movable ORF collection. *Genes Dev.* **19,** 2816–2826
35. Oganesyan, N., Ankoudinova, I., Kim, S. H., and Kim, R. (2007) Effect of osmotic stress and heat shock in recombinant protein overexpression and crystallization. *Protein Expr. Purif.* **52,** 280–285
36. Poor, C. B., Wegner, S. V., Li, H., Dlouhy, A. C., Schuermann, J. P., Sanishvili, R., Hinshaw, J. R., Riggs-Gelasco, P. J., Outten, C. E., and He, C. (2014) Molecular mechanism and structure of the *Saccharomyces cerevisiae* iron regulator Aft2. *Proc. Natl. Acad. Sci. U.S.A.* **111,** 4043–4048
37. Vijayakumar, A., Vijayaraj, P., Vijayakumar, A. K., and Rajasekharan, R. (2016) The *Arabidopsis* ABHD11 mutant accumulates polar lipids in

leaves as a consequence of absent acylhydrolase activity. *Plant Physiol.* **170,** 180–193
38. Yadav, K. K., Singh, N., and Rajasekharan, R. (2015) PHO4 transcription factor regulates triacylglycerol metabolism under low-phosphate conditions in *Saccharomyces cerevisiae*. *Mol. Microbiol.* **98,** 456–472
39. Simons, B., Kauhanen, D., Sylvänne, T., Tarasov, K., Duchoslav, E., and Ekroos, K. (2012) Shotgun lipidomics by sequential precursor ion fragmentation on a hybrid quadrupole time-of-flight mass spectrometer. *Metabolites* **2,** 195–213
40. Huang, H., Taraboletti, A., and Shriver, L. P. (2015) Dimethyl fumarate modulates antioxidant and lipid metabolism in oligodendrocytes. *Redox Biol.* **5,** 169–175
41. Rose, M., and Botstein, D. (1983) Construction and use of gene fusions to lacZ (β-galactosidase) that are expressed in yeast. *Methods Enzymol.* **101,** 167–180
42. van Attikum, H., Fritsch, O., Hohn, B., and Gasser, S. M. (2004) Recruitment of the INO80 complex by H2A phosphorylation links ATP-dependent chromatin remodeling with DNA double-strand break repair. *Cell* **119,** 777–788
43. Laha, S., Das, S. P., Hajra, S., Sanyal, K., and Sinha, P. (2011) Functional characterization of the *Saccharomyces cerevisiae* protein Chl1 reveals the role of sister chromatid cohesion in the maintenance of spindle length during S-phase arrest. *BMC Genet.* **12,** 83
44. Lewandowska, A., Gierszewska, M., Marszalek, J., and Liberek, K. (2006) Hsp78 chaperone functions in restoration of mitochondrial network following heat stress. *Biochim. Biophys. Acta* **1763,** 141–151